Warming up the Universe: JWST deep lensing field as a tool to constrain Fundamental Physics

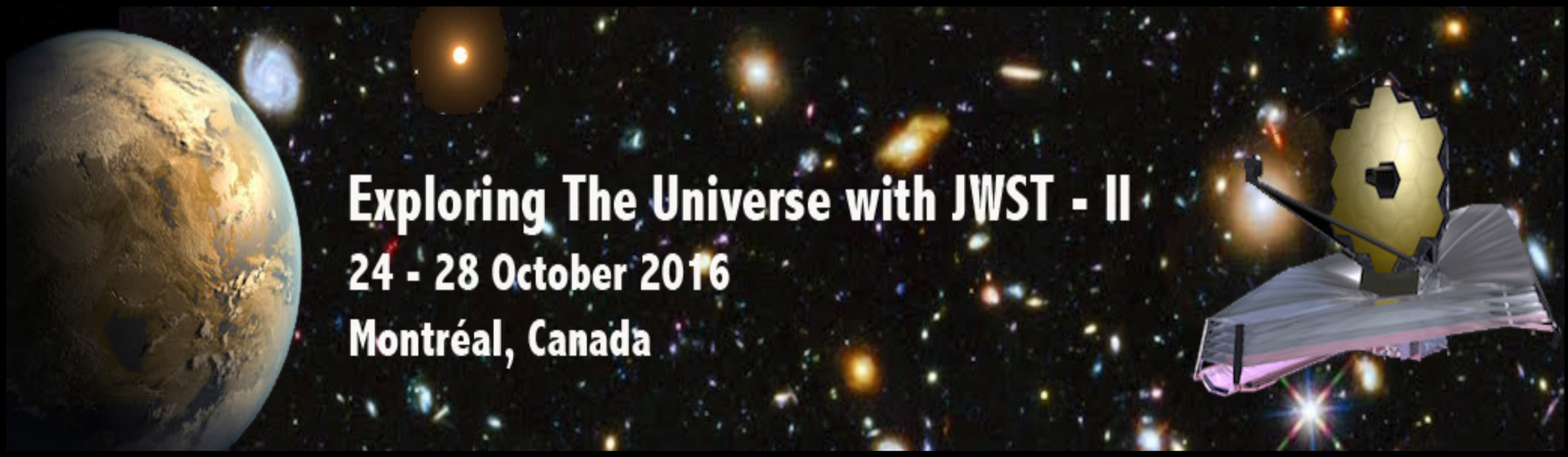

Andrea Grazian (INAF-OAR)

N. Menci, M. Castellano, M. Meneghetti, N. Sanchez, A. Merle, M. Totzauer, A. Schneider

October 28th, 2016 Montreal (Canada)

“Exploring the Universe with JWST-II” Conference

CRITICAL ISSUES CONCERNING COLD DARK MATTER AT SMALL GALACTIC SCALES

Overabundance of low-mass objects

i) abundance of faint galaxies

ii) abundance of satellite DM halos

iii) density profiles

iv) the M_*-M_{halo} relation

v) star formation histories of dwarfs

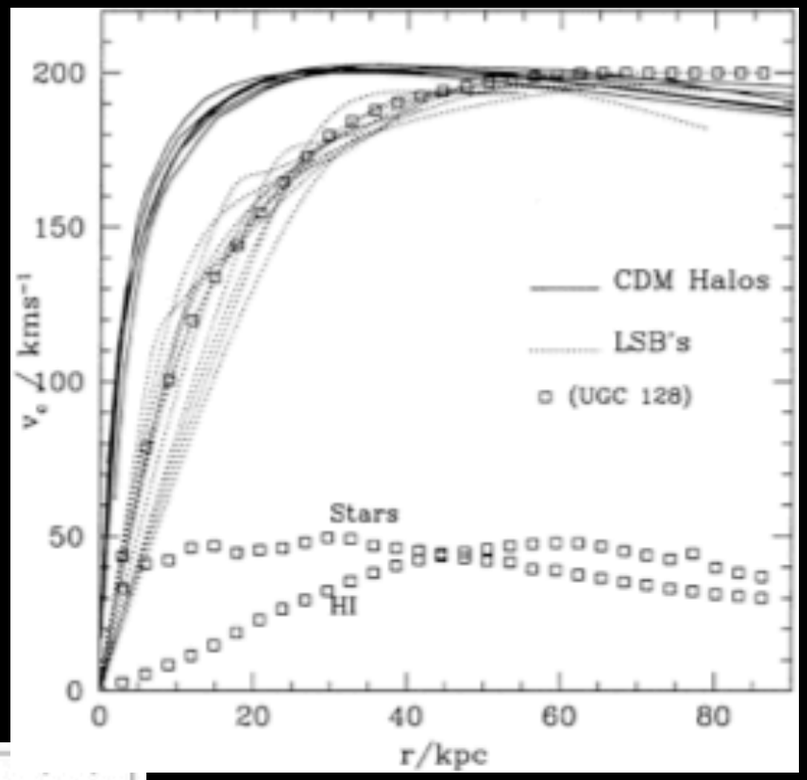

Moore et al. 2002

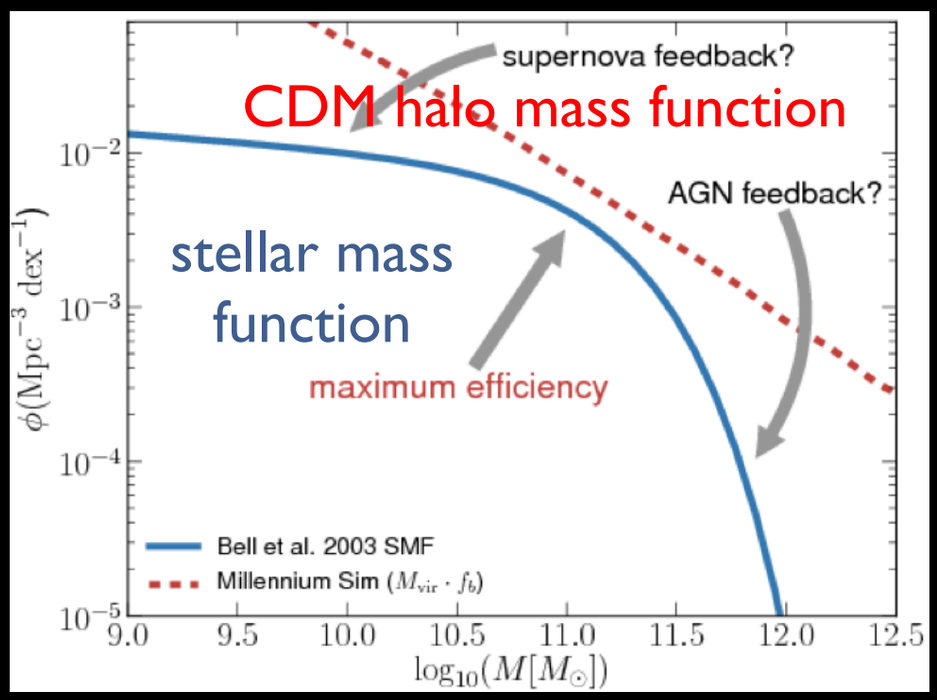

Mutch 2013

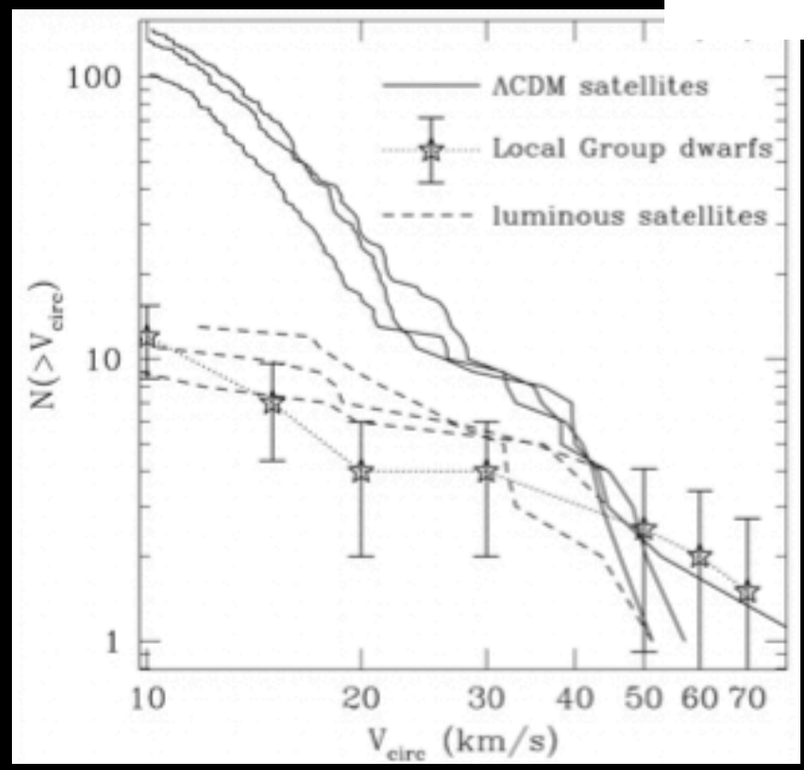

Kravtsov, Klypin, Gnedin 2004

Solutions from Feedback Processes

i) the abundance of satellite galaxies

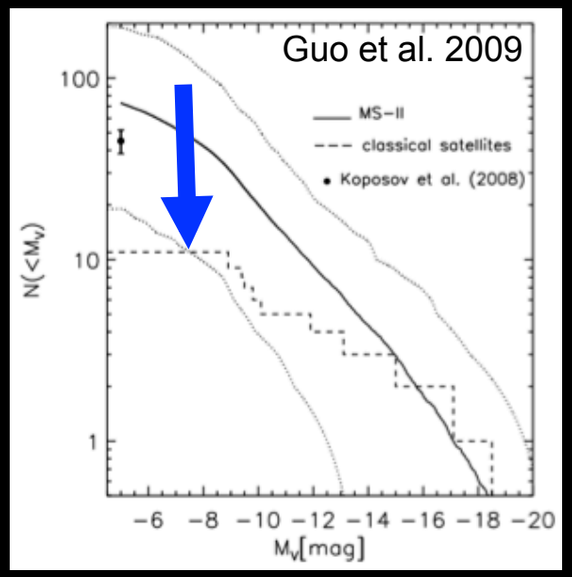

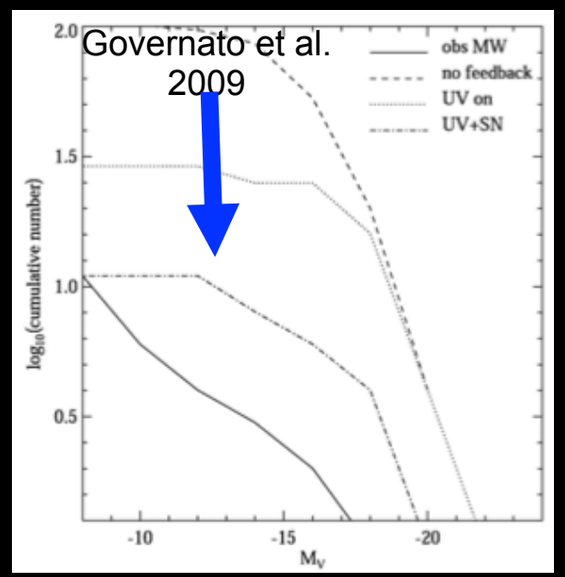

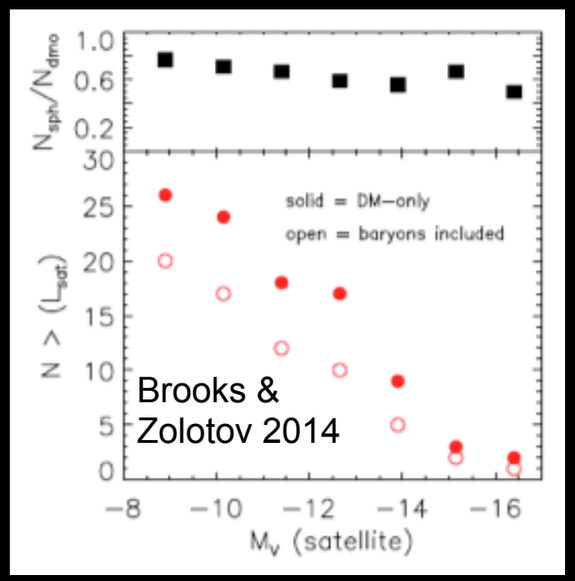

ii) the density profiles

A proposed solution at low redshift

"... The rapid fluctuations caused by episodic feedback progressively pump energy into the DM particle orbits, so that they no longer penetrate to the center of the halo" (Weinberg et al. 2013, Governato et al. 2012)

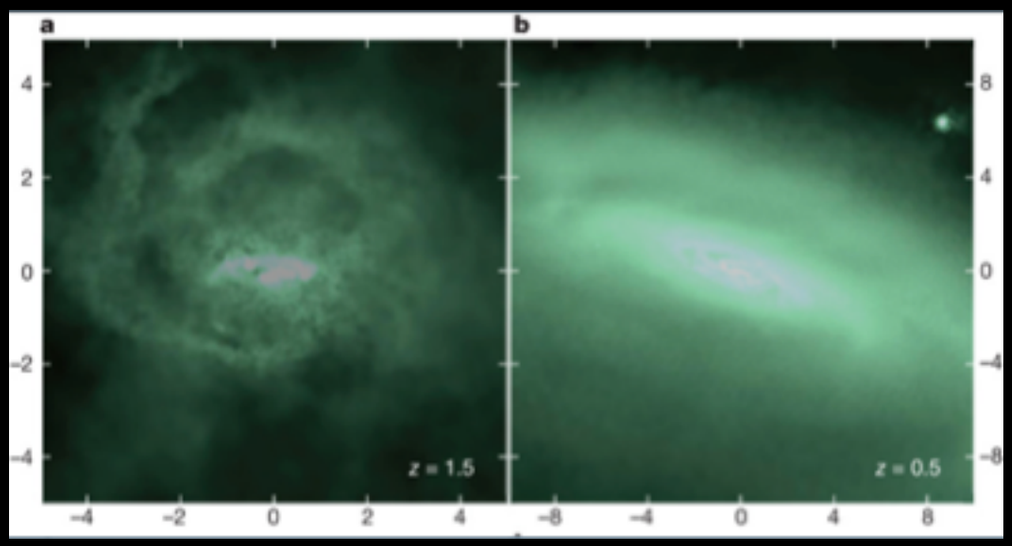

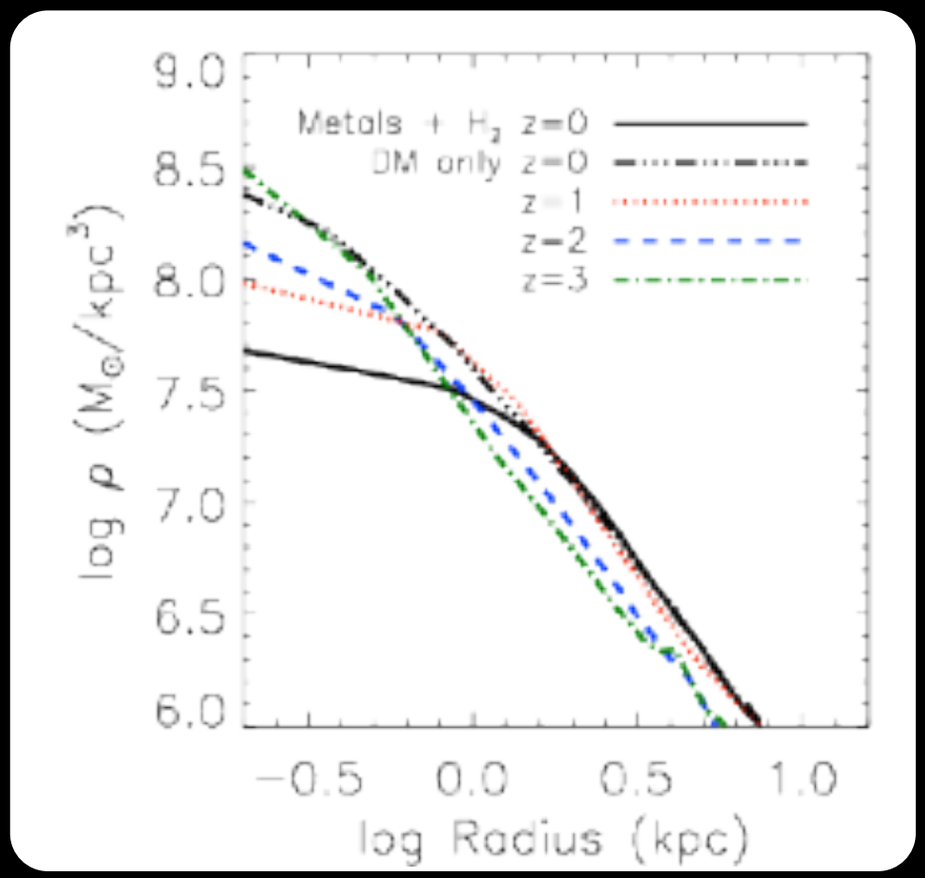

see Brookes' talk

Problems with Solutions based on Feedback

1: Profiles and Abundances of low-mass galaxies at high redshifts

- Steeper central profiles are expected at z>1

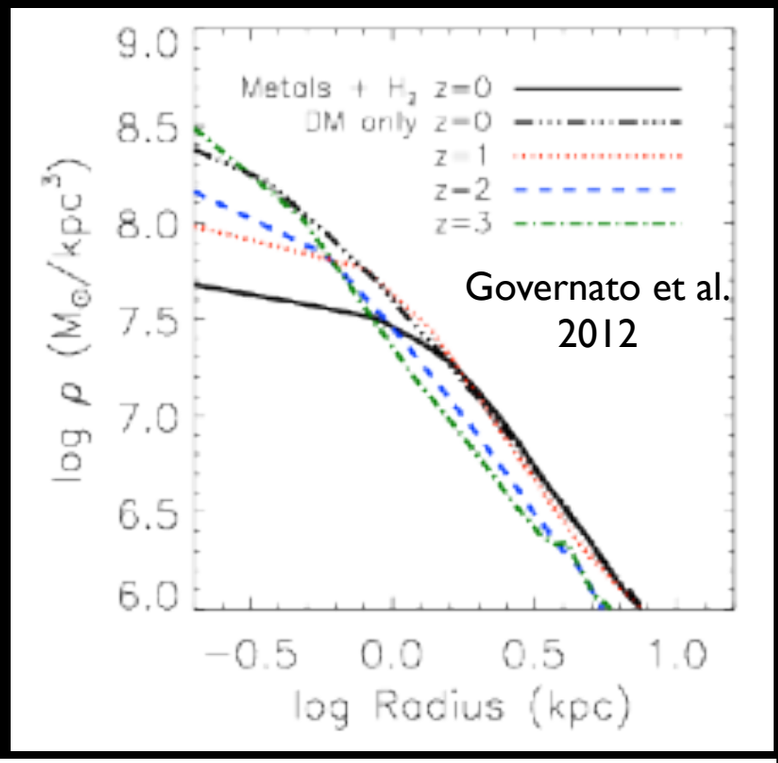

- Steeper luminosity and mass functions are expected at z>1

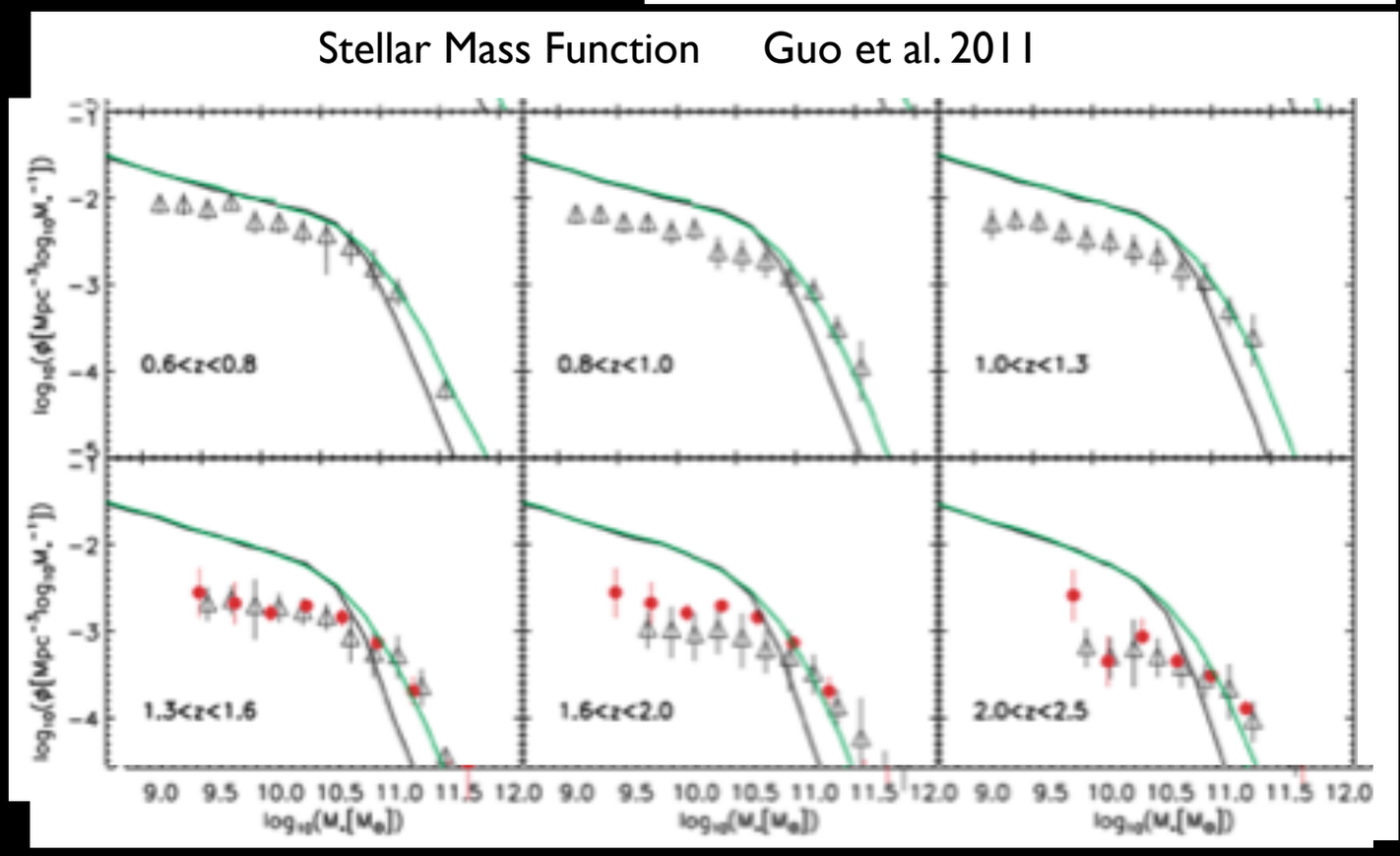

SOLUTIONS BASED ON ASSUMED DARK MATTER MODEL

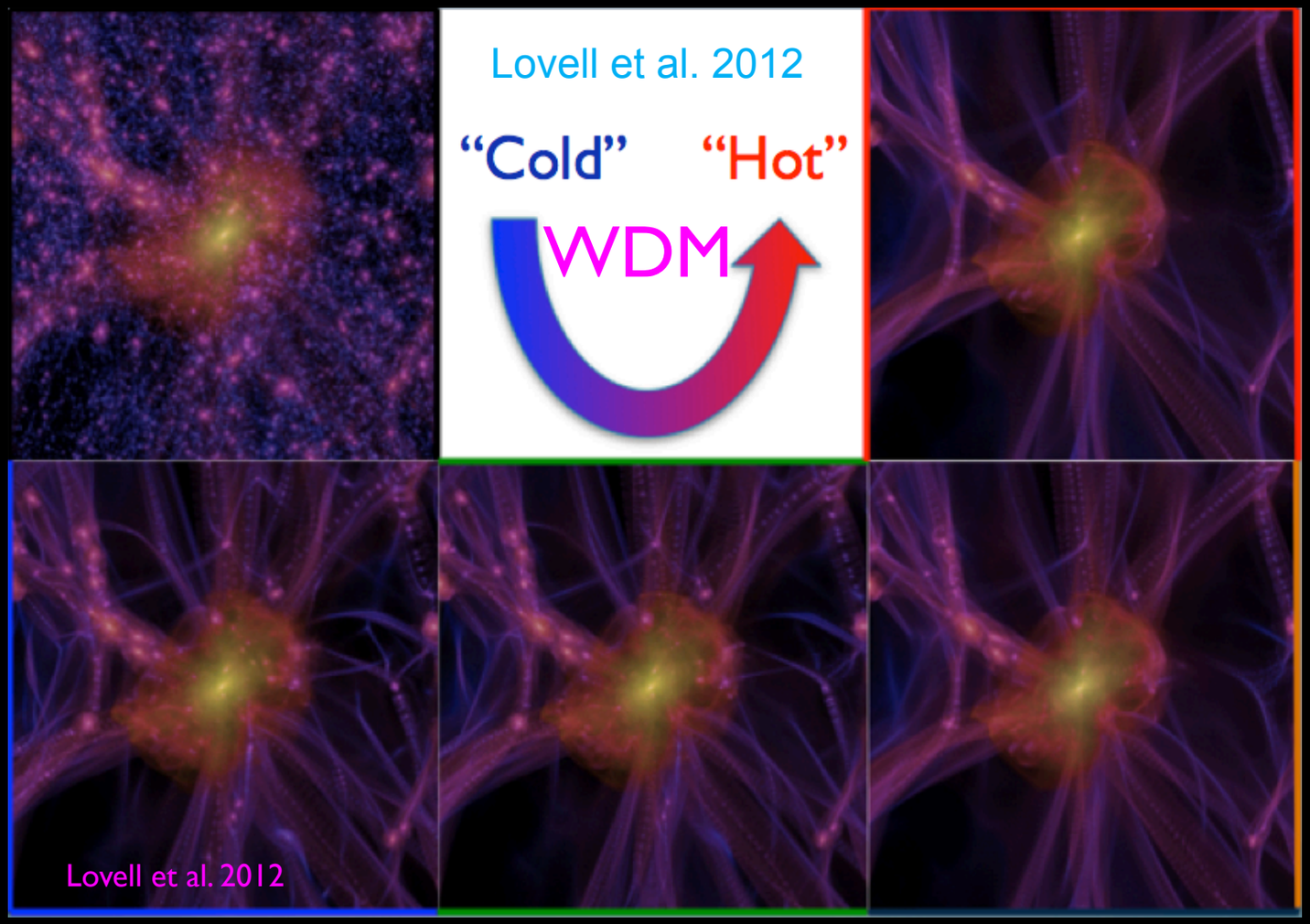

Dissipation,
free-streaming scale

See Mesinger talk

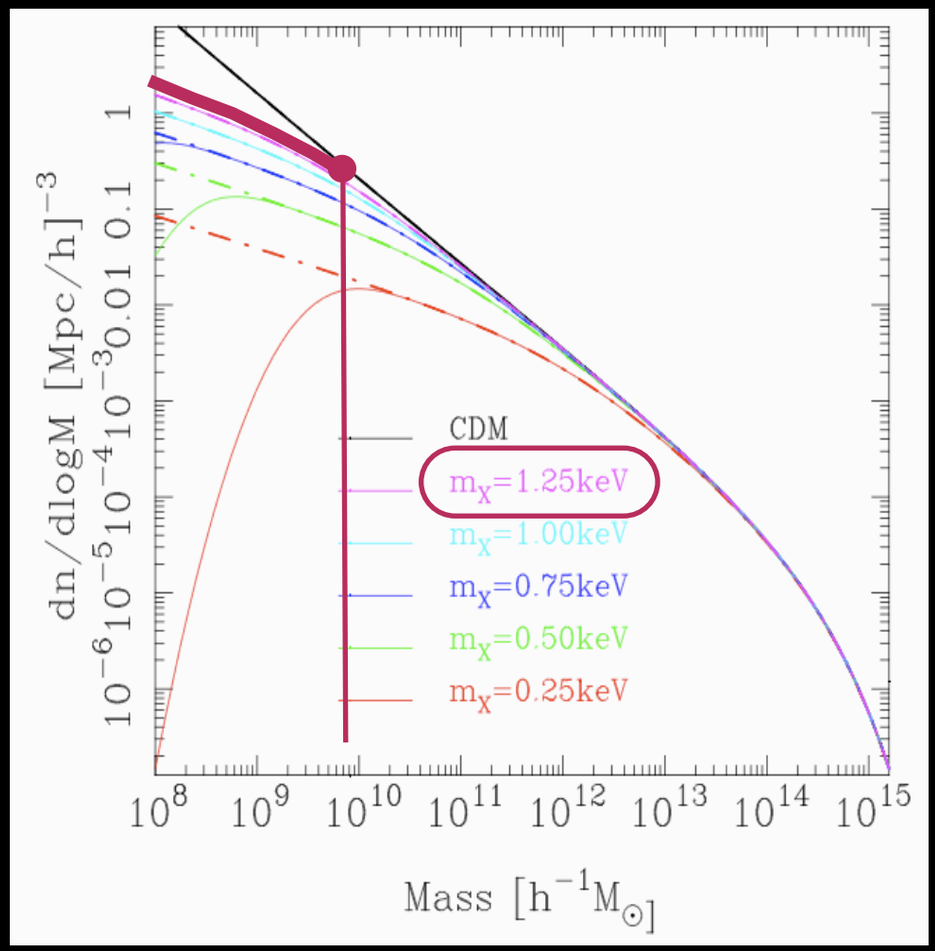

Compared to CDM, in WDM models the abundance of low-mass structures is suppressed below the half mode mass

Dissipation, free-streaming scale

$$r_{fs} = \int_0^t \frac{v(t)}{R(t)}$$

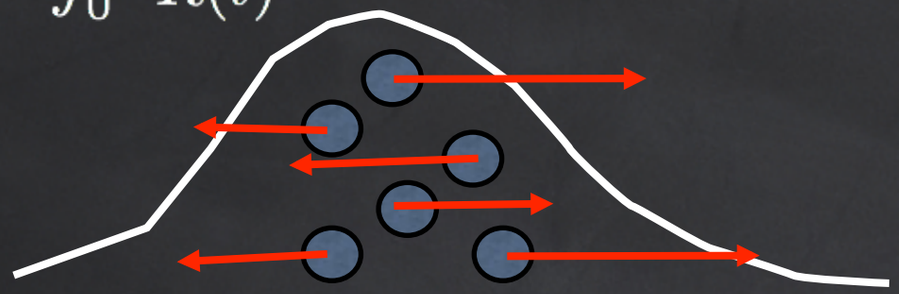

$$\sigma_\chi \propto a^{-1} m_\chi^{-1/2}$$

$$M_{fs} = 4 \times 10^{15} \left(\frac{m_\nu}{30 \text{ eV}} \right)^{-2} M_\odot$$

Lighter and faster Warm Dark Matter particles stream out of density perturbations.

CDM: the free streaming length is much smaller than any scale involved in galaxy formation ($\ll$Mpc)

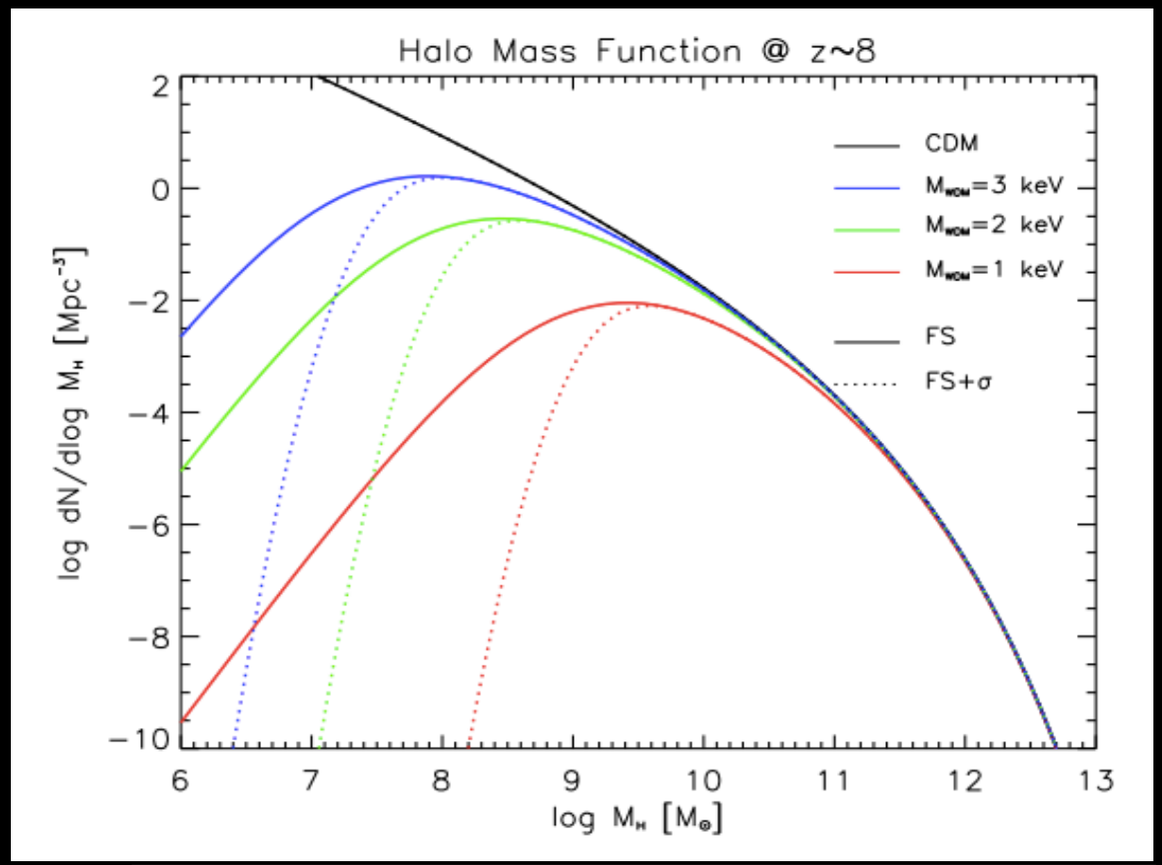

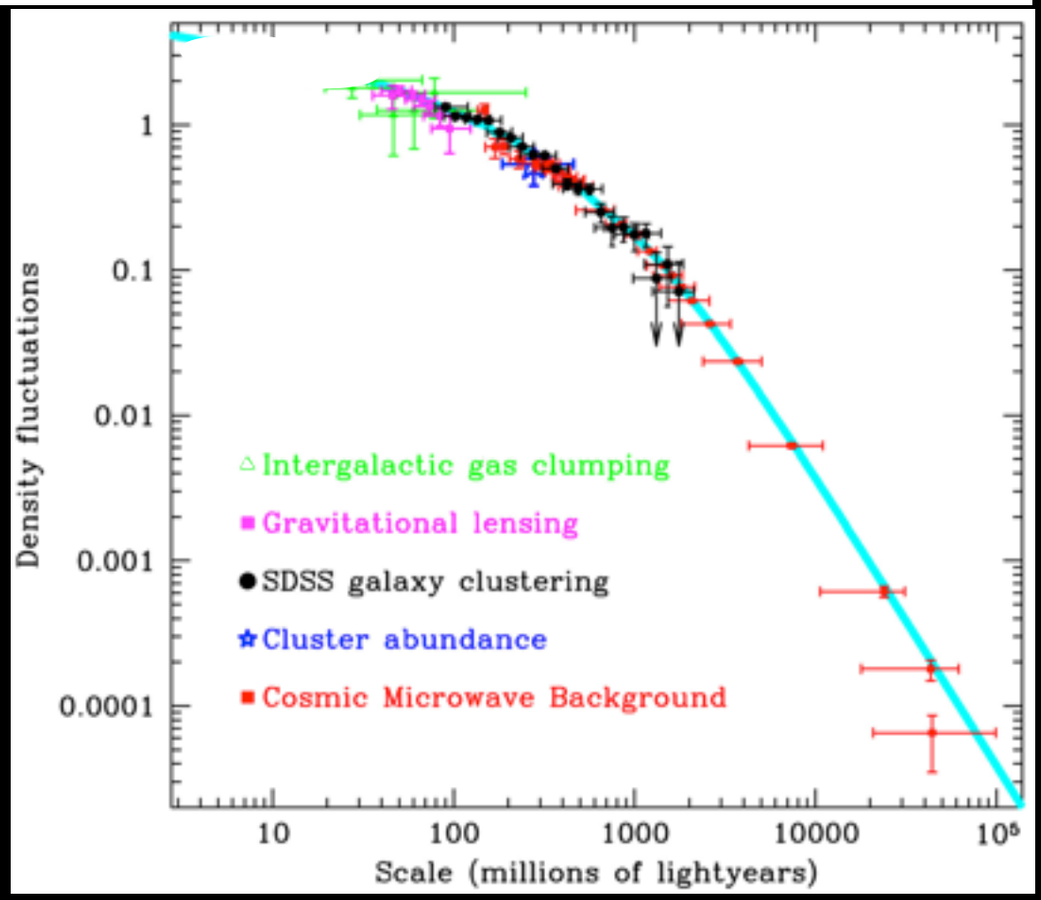

WDM models with m_X=1-4keV can provide a solution to

Density profiles & Rotation curves in WDM (De Vega et al. 2014)

Luminosity and Mass Functions at z<1

Color Distributions

Abundance of low-mass satellites

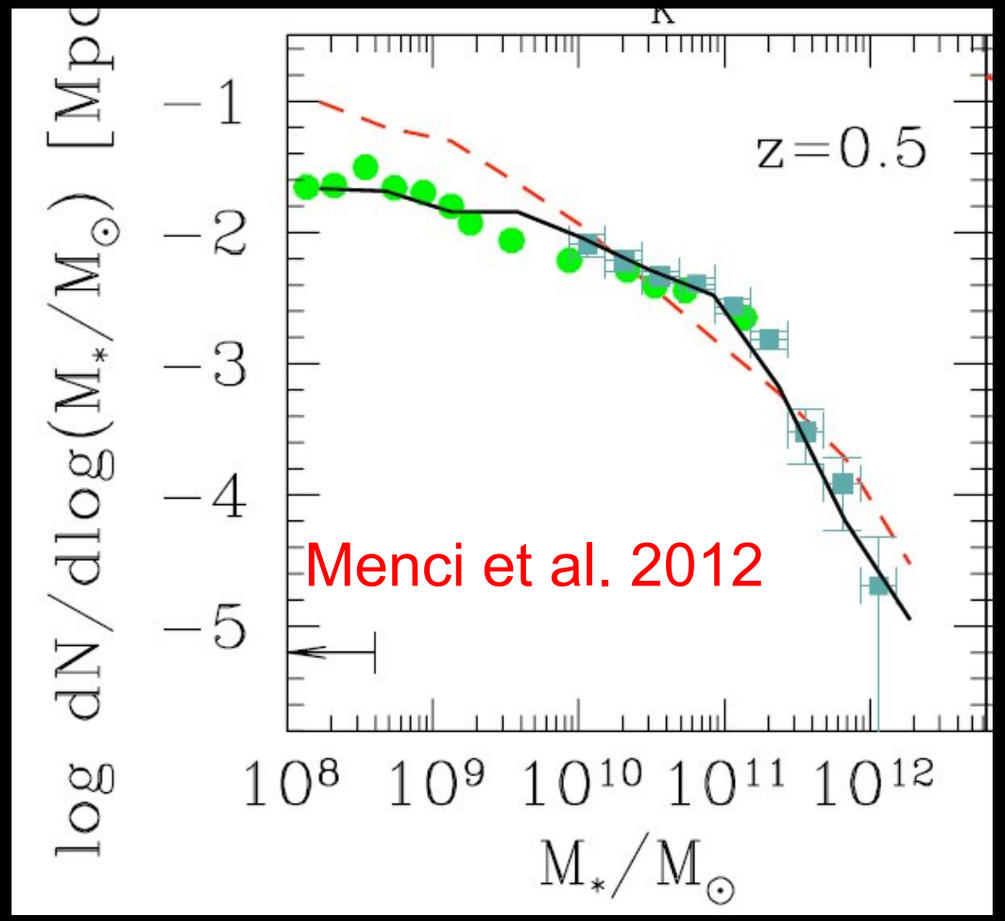

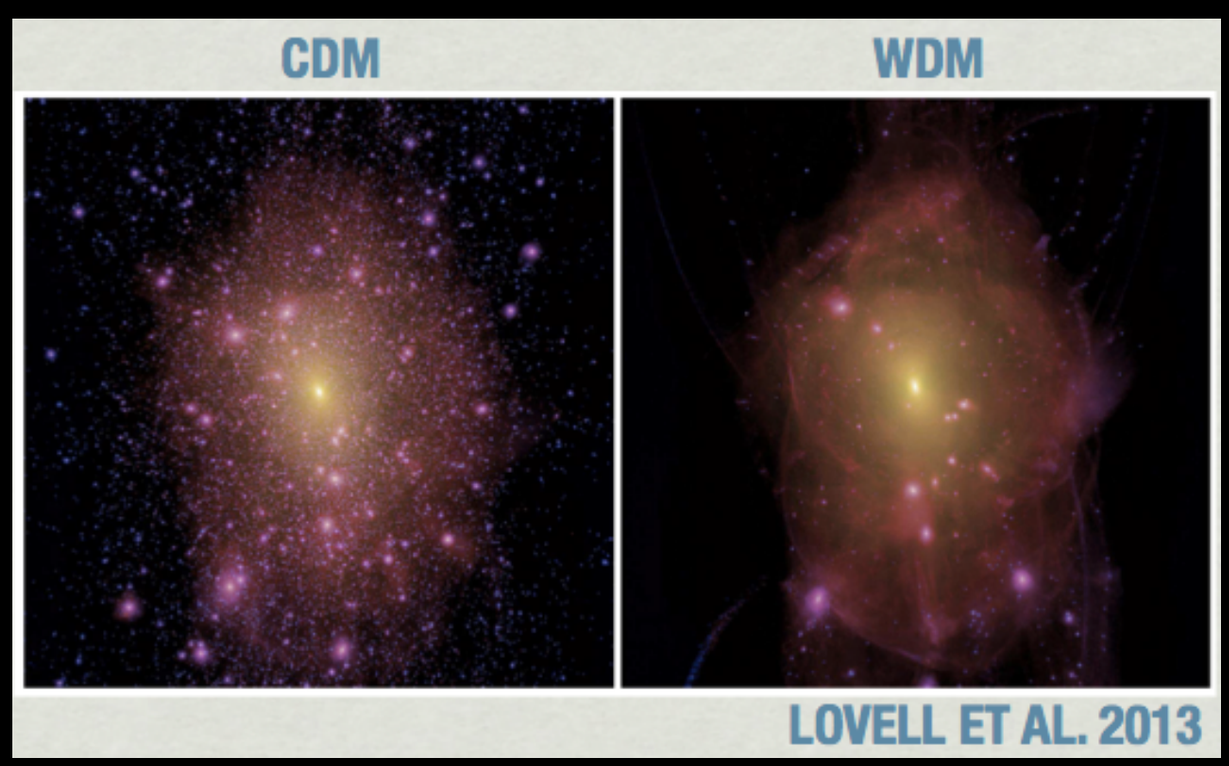

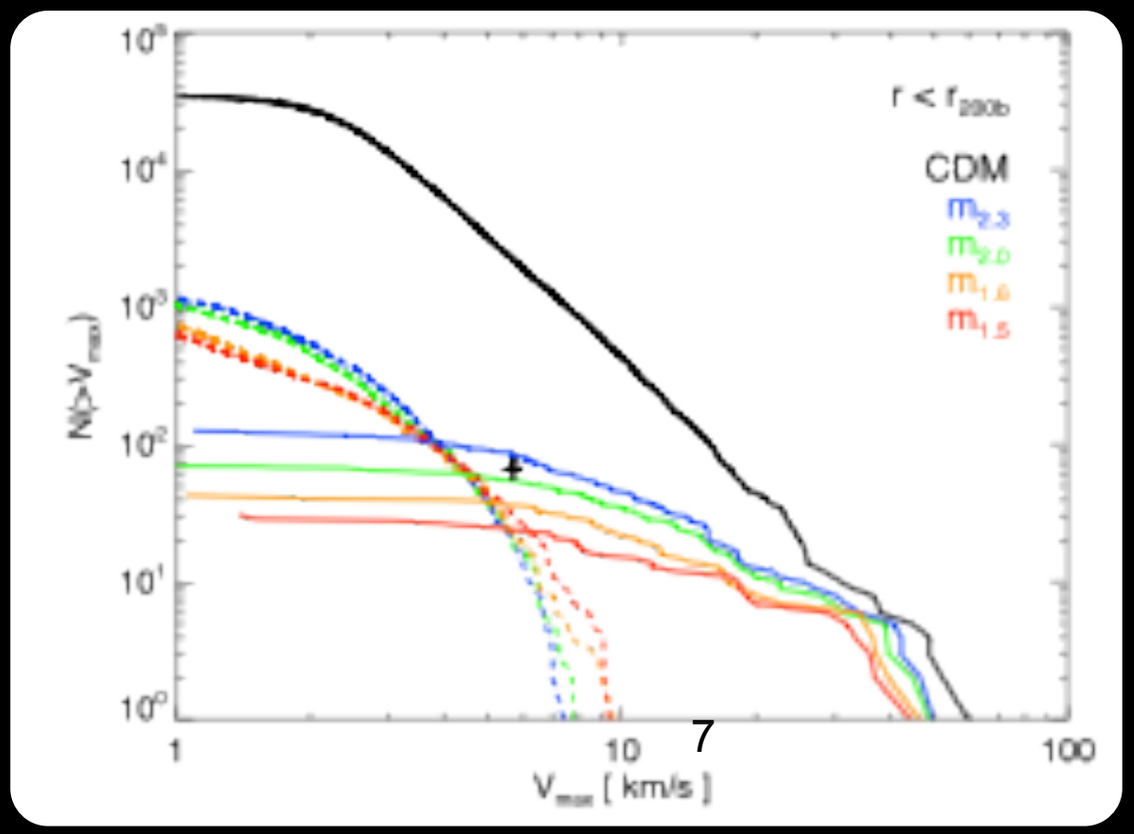

Maccio et al. 2012, Benson et al. 2013, Dayal, Mesinger, Pacucci 2014, Herpich et al.2014, Governato et al. 2014, Kennedy et al. 2015 Bose et al. 2016, Chau, Mayer, Governato 2016

WDM particle mass: limits from the Ly-α forest vs. Hydro-Simulations

Viel et al. 2005; 2013

m_{WDM}>3.3 keV	Thermal relics WDM
m_{ν}>12 keV	Sterile ν WDM (DW) Dodelson-Widrow

Results subject to further investigations

(Garzilli et al. 2015): WDM>2keV

Still affected by the difficult-to-characterize physics of intergalactic gas. Degeneracy between WDM effects and Jeans and Doppler broadening of the absorption lines. These are affected by the IGM temperature.

WDM halos are 10^{68} times heavier (10^5 $M_\odot$) than the real WDM particles (~keV). This makes difficult to infer the initial velocity distribution of the effective particles from the known initial velocity distribution of the real WDM particles (Lovell et al. 2012, 2014; Maccio` et al. 2012; Viel et al. 2013).

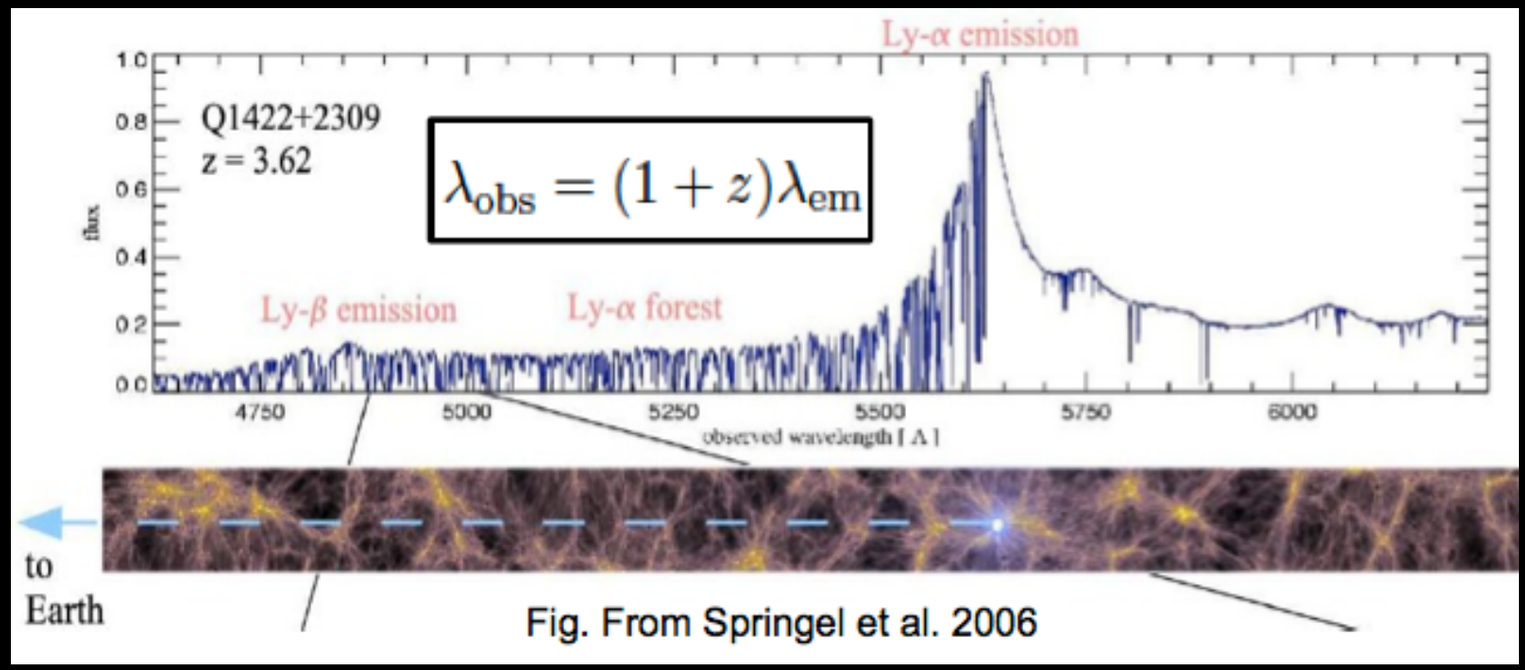

Fig. From Springel et al. 2006

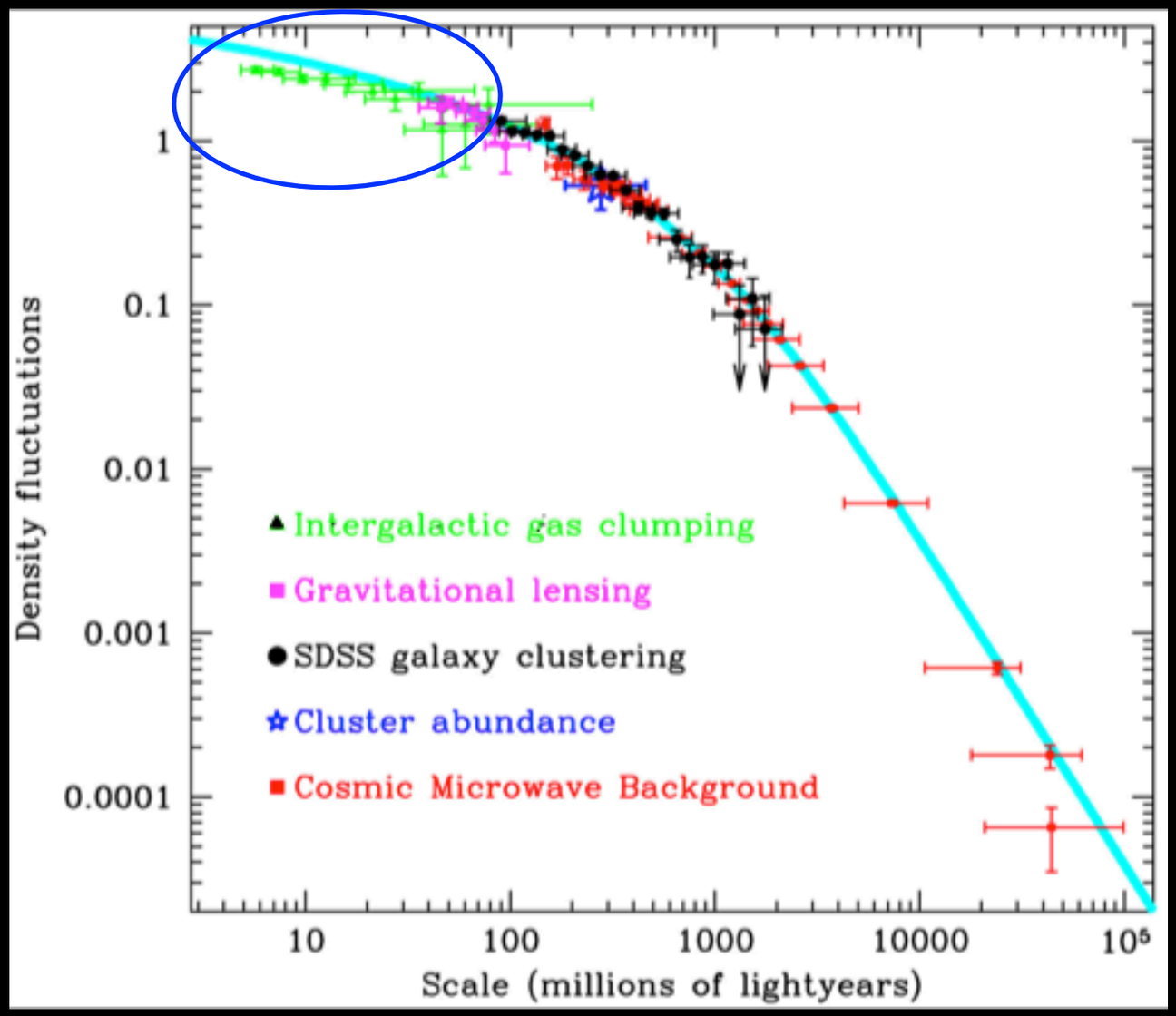

Constraining the WDM candidate mass through the abundance of low-mass galaxies

Structure formation in WDM models is suppressed on small mass scales.

Small mass galaxies are the first to form.

A powerful probe for these scenarios is the abundance of high-z galaxies.

Observed galaxy densities larger than the maximum predicted abundance of a given WDM model would rule out the corresponding WDM particle mass

Delicate issue: relate UV luminosity of observed galaxies to the mass of the host DM halo.

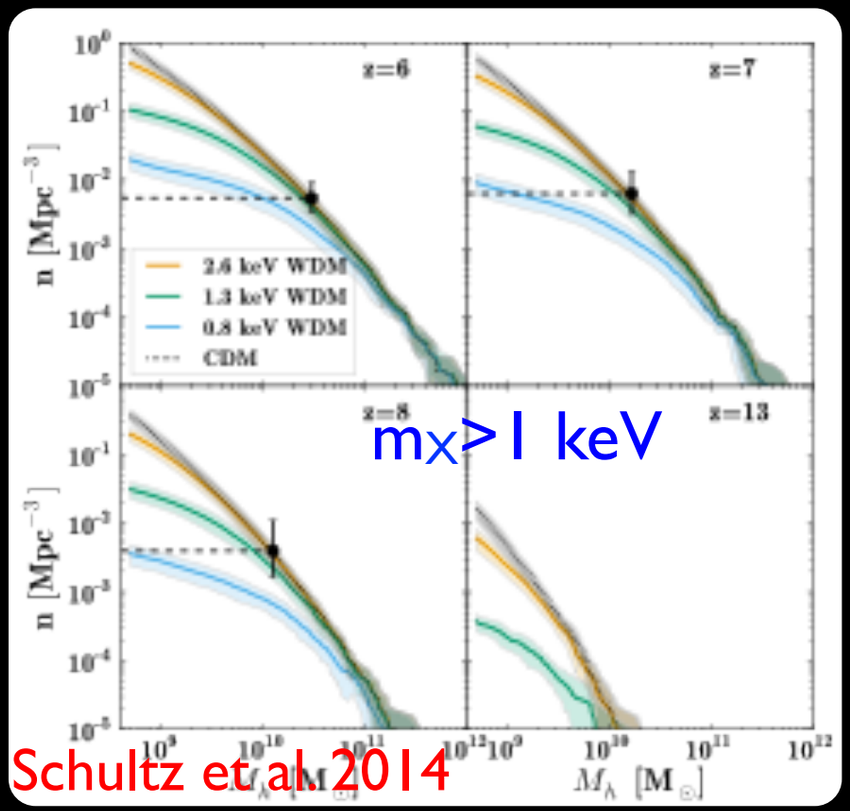

m_X>1 keV

Schultz et al 2014

Probing WDM mass of ~ 2 keV requires reaching M_{UV}≈ -13

much, much deeper than present limit of HST

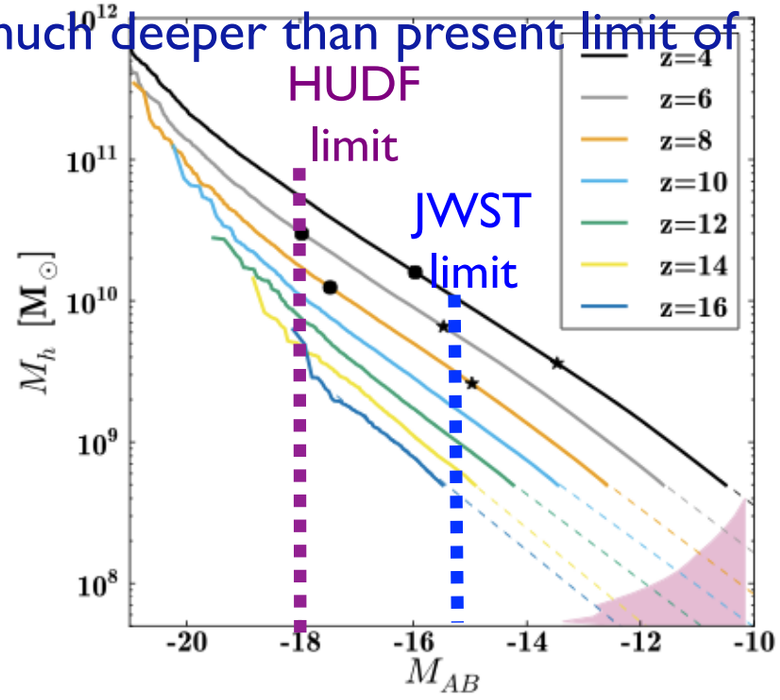

Blank fields

HUDF Magnitude limit mag=30.
This corresponds to M_{UV}=-18 at z=6.

Hubble Frontier Fields

Abell 2744 Cluster

Clusters as lensing telescopes

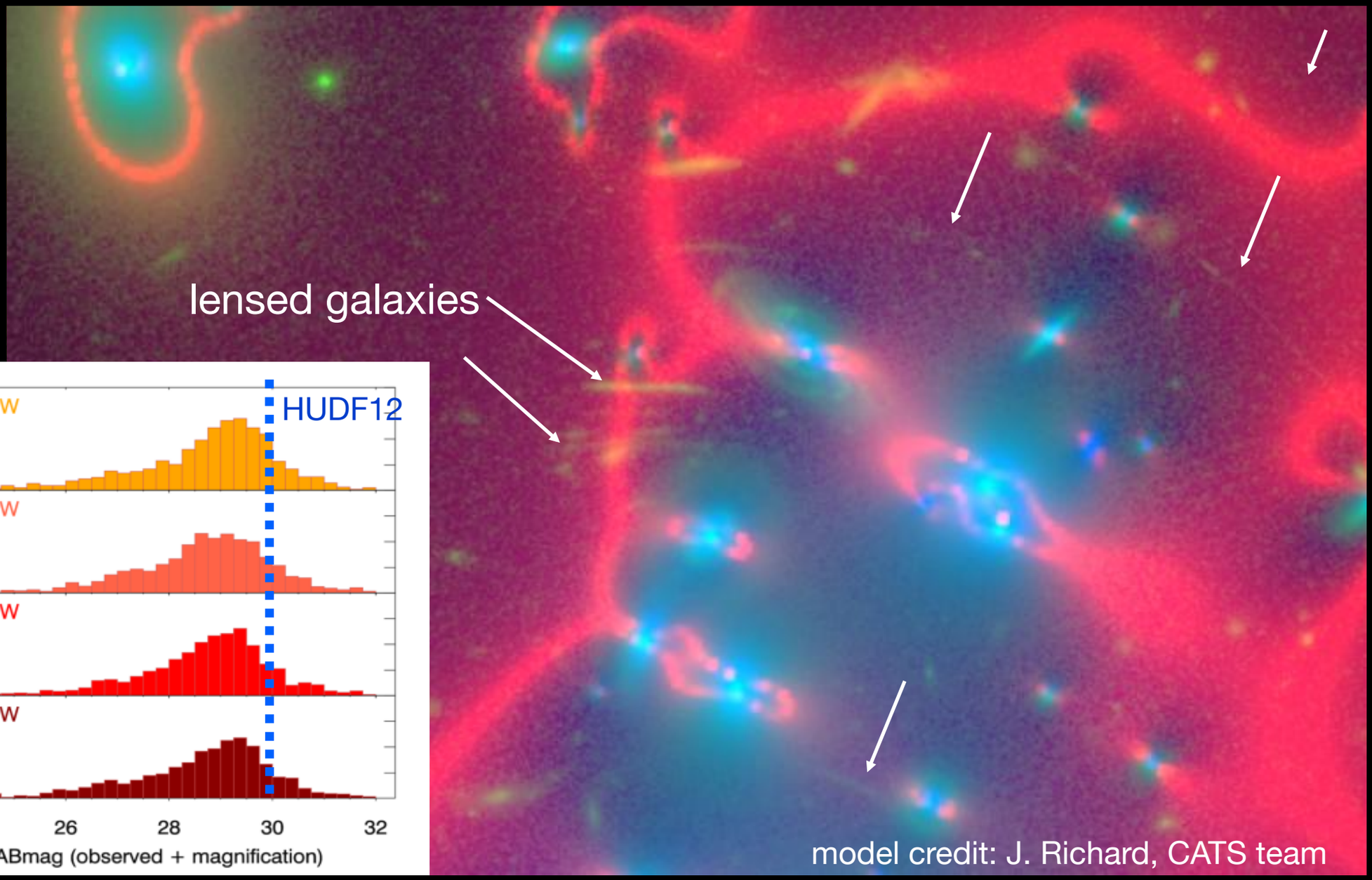

background galaxies are magnified by factors up to ~10-20,
providing the deepest yet view of the Universe

intrinsically faintest Frontier Fields galaxies ~2.5 magnitudes fainter than HUDF12

Original slide by Jennifer Lotz

Abundance of z=6 galaxies down to M_{UV}=-12.5

Livermore, Finkelstein, Lotz 2016

Based on 2 HFF lensing clusters Abell 2744 and MACS 0416

164 galaxies at z~6

Menci, Grazian et al. 2016

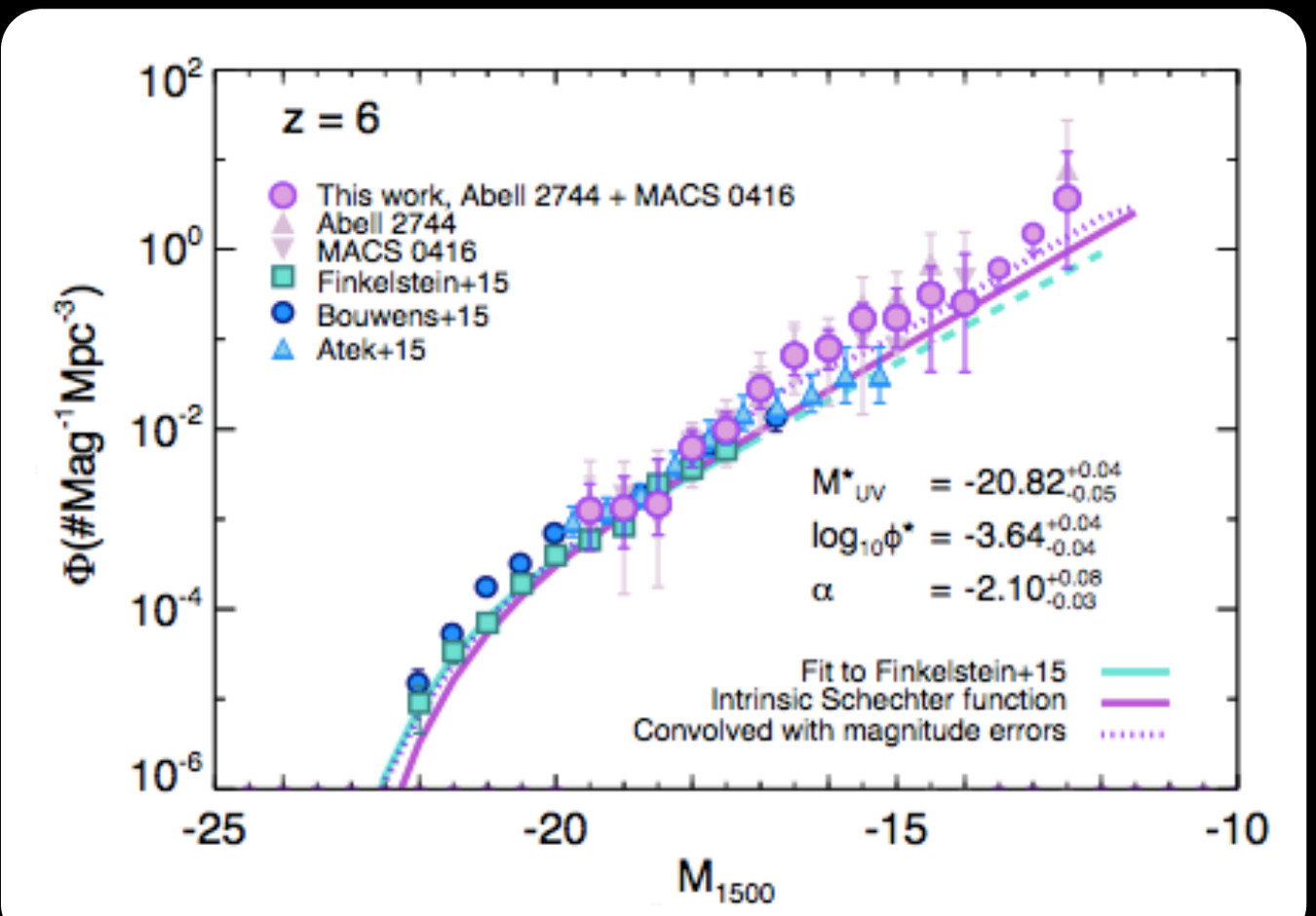

Lensing magnifications >50X

Magnifications have been derived by adopting the full range of possible lens models produced for the HFF by seven independent groups who used different assumptions and methodologies.

1. Starting from observed luminosity function of LFL16, we run 10^7 Monte Carlo extractions of galaxies according to the observed distribution and with an uncertainty provided by the observed error bars.
2. Compute the cumulative number density of galaxies down to the faintest mag bin: # of galaxies/Mpc^3
at different confidence levels.
Cumulative number density does not depend on DM Mass/Light ratio

Best fit	$\log \Phi_{obs}/Mpc^3 = 0.54$
1 σ	$\log \Phi_{obs}/Mpc^3 = 0.26$
2 σ	$\log \Phi_{obs}/Mpc^3 = 0.01$
3 σ	$\log \Phi_{obs}/Mpc^3 = -0.36$

Result: m_X>2.4 keV (thermal relic mass)

When compared with maximum number density of DM halos in WDM models

we find a limit m_X>3 keV (1 σ), m_X>2.4 keV (2 σ) thermal relics

The tighter limits on mX derived so far independently of astrophysical processes

Menci, Grazian, et al. 2016

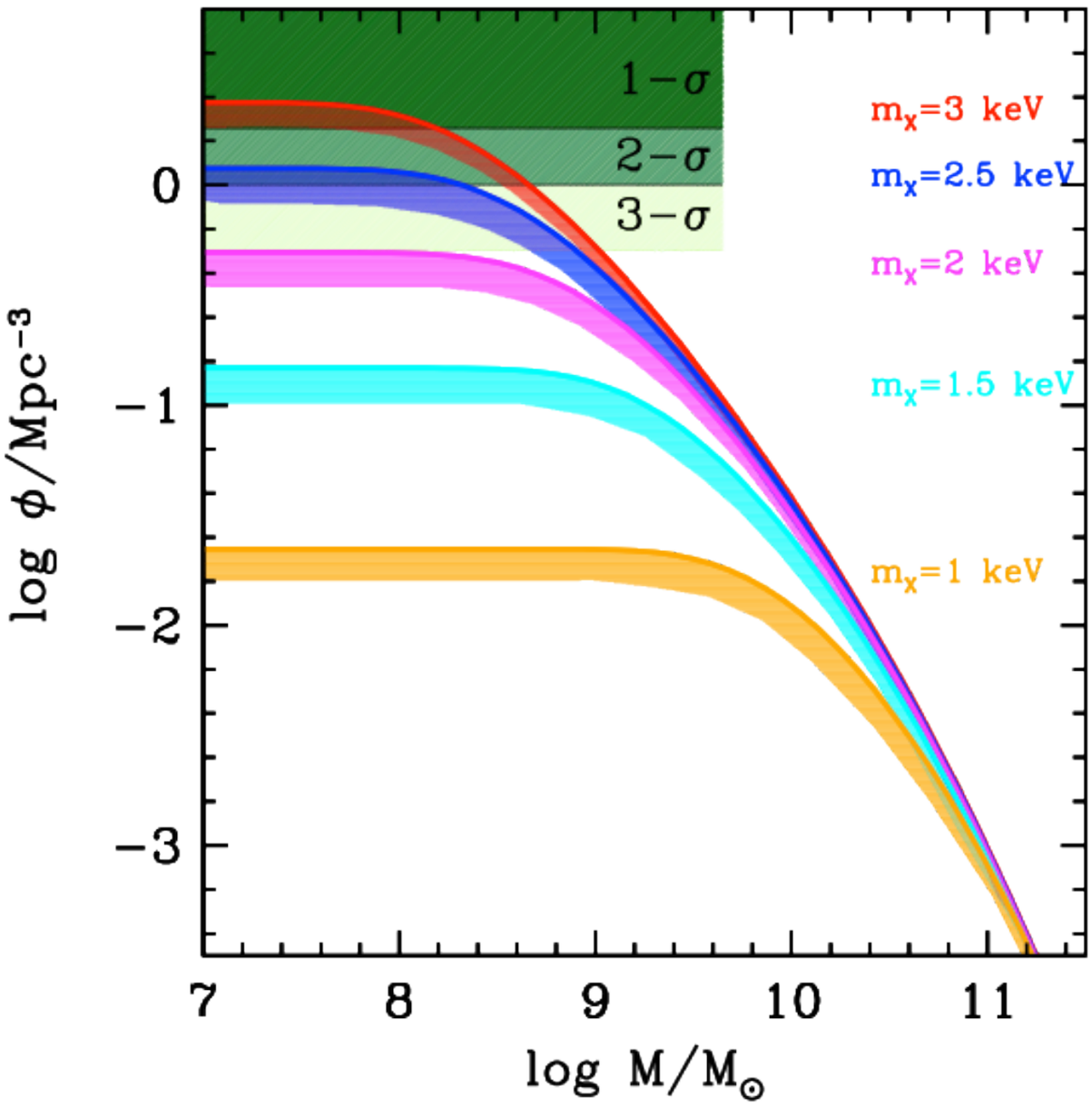

No matter what are the gas and star formation processes involved in galaxy formation: visible galaxies cannot outnumber their host DM halos

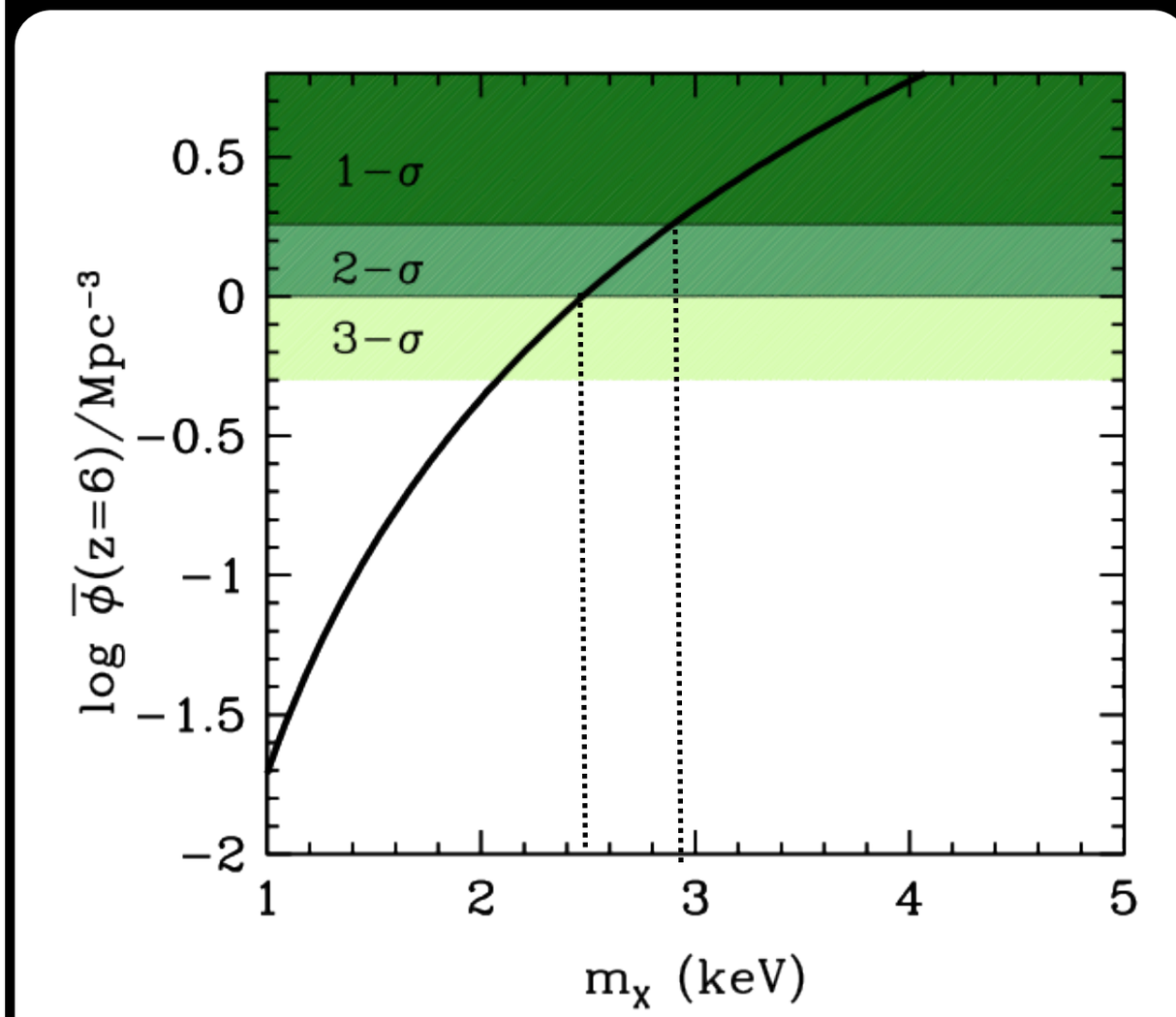

Comparison with previous limits based on galaxy abundances

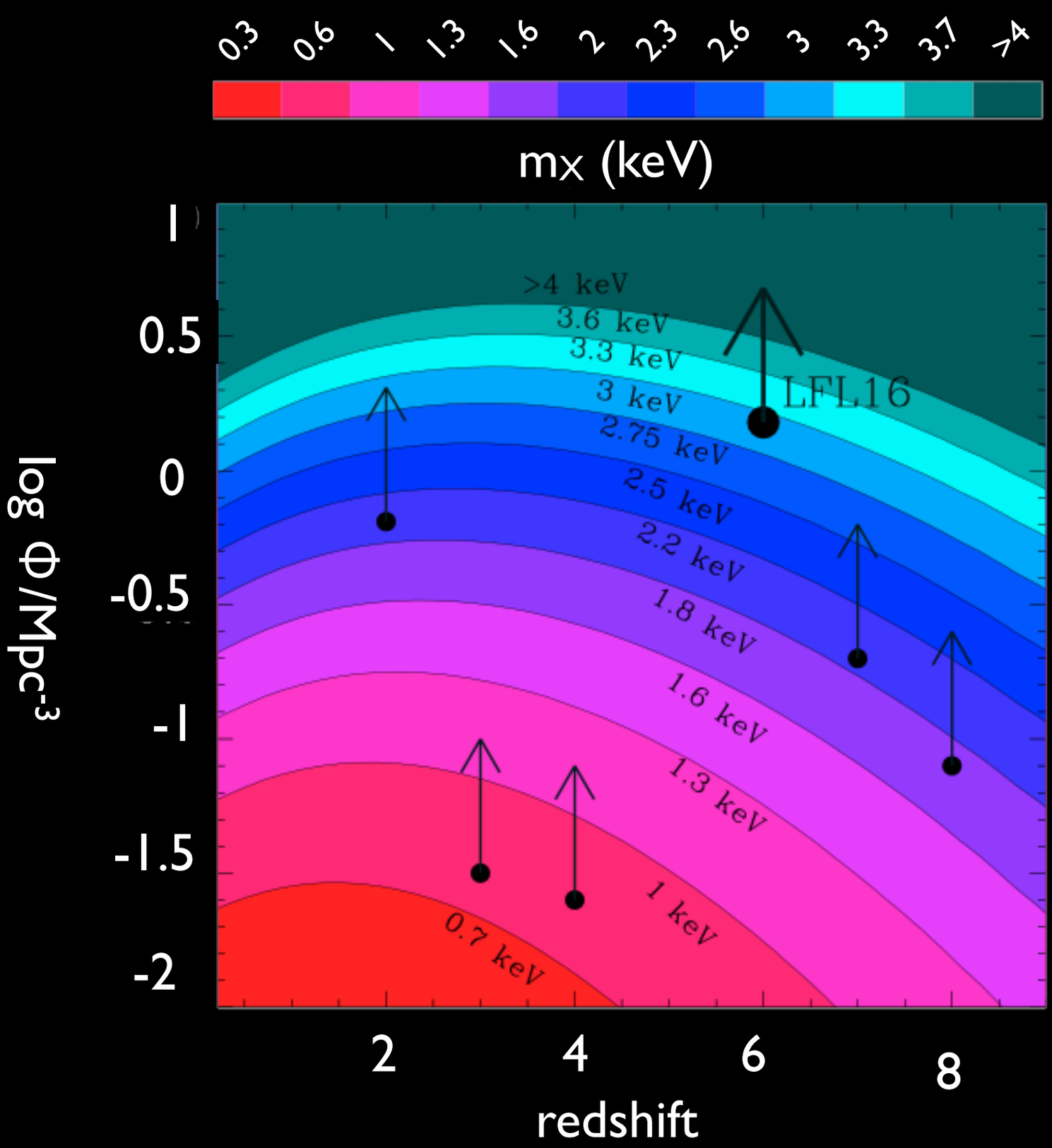

Data from

Alavi et al. 2015 z=2

Parsa et al. 2015 z=3-4

Livermore et al. 2016 z>6

Menci, Grazian et al. 2016

A robust result: theory

Lower values of m_X=3keV do not provide the observed abundance.

Note: baryonic processes can make the LF flatter but not steeper !

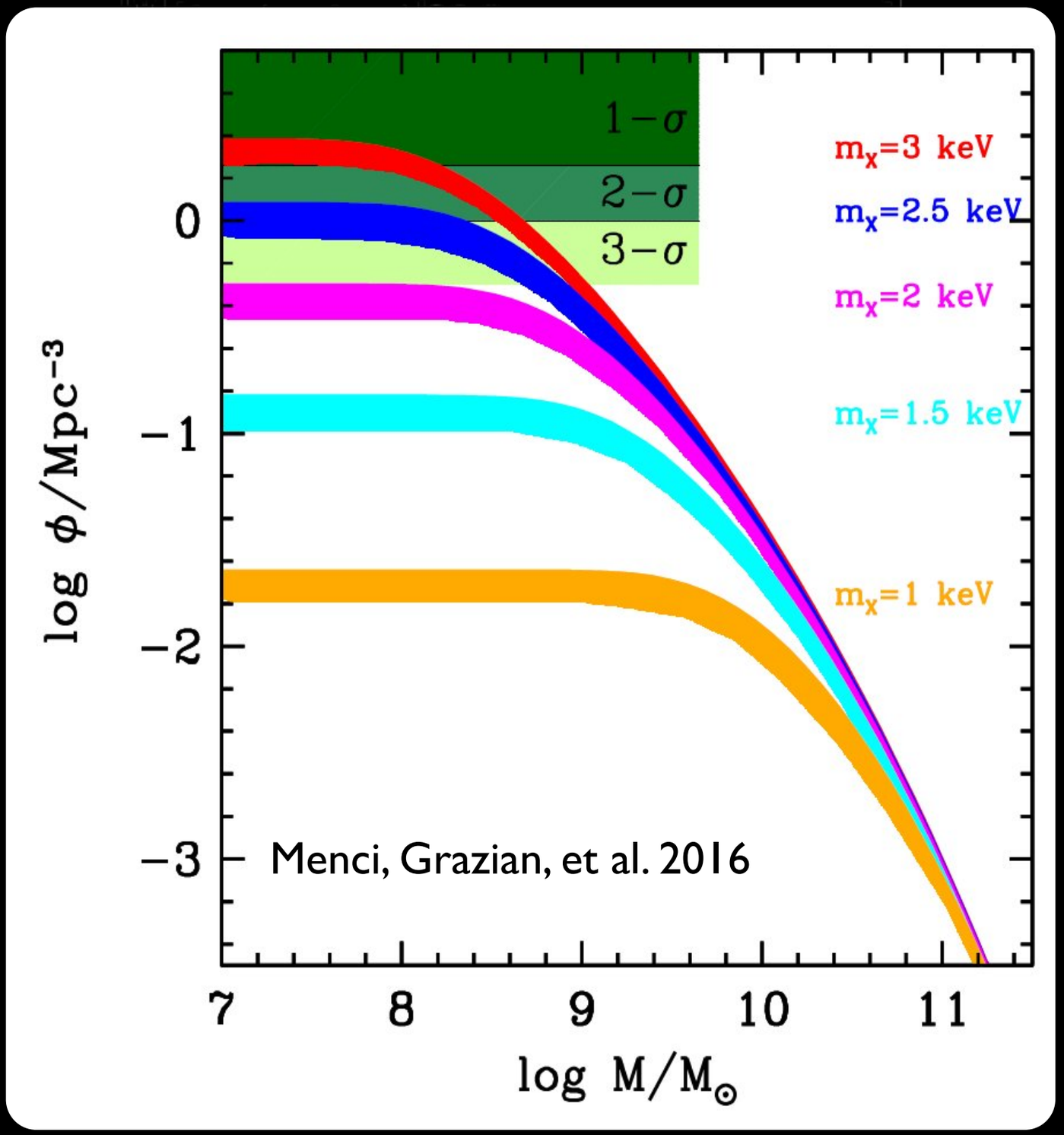

The result is robust with respect to:

1-The effect of baryonic processes included in η. Observations probe the mass function in the mass range around the half-mode mass where the DM mass functions are characterized by a maximum value.

2-The modeling of residual DM dispersion velocities. Their would yield a sharper decrease of the mass function at small masses (see, e.g., Benson et al. 2013), thus yielding tighter constraints.

3-The kind of DM clumps hosting the UV emitting galaxies. In fact, the upper boundaries of the solid filled regions correspond to predictions including also proto-halos.

4-The possible effects of UV background and reionization. Such effects would further suppress the abundance of galaxies in low-mass halos (Sawala et al. 2015).

5-The collapse threshold: conservatively assume spherical collapse model. elliptical collapse yields even stronger limits

Caveats: observations

Present constraints on WDM mass are based on the z=6 Luminosity Function of Livermore, Finkelstein & Lotz 2016.

Recent papers (e.g. Bouwens et al. 2016) stressed the importance of galaxy sizes and careful analysis of lensing models at faint intrinsic luminosities.

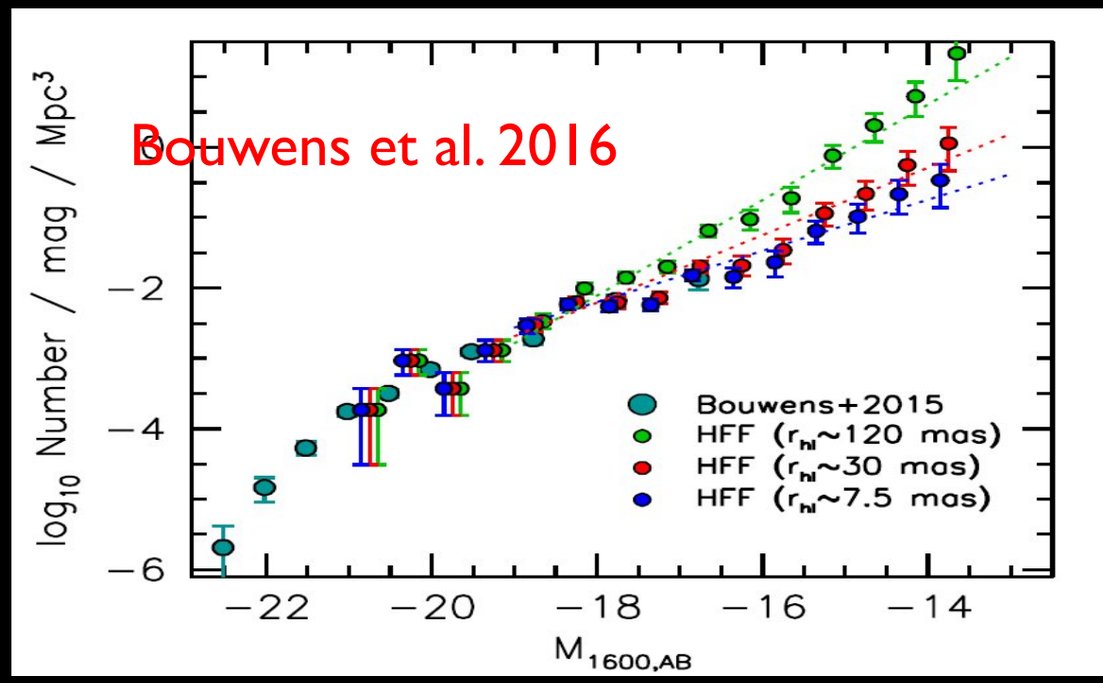

But see Kawamata et al. 2015.
At z=6 and Muv=-21, re=1 kpc (half light radius). Assuming size-luminosity relation of Grazian et al. 2012 L^-0.5: at Muv=-12.5 re=30 pc expected, with log-normal tail at larger radii (sigma_re~60 pc).
Thus the assumption of Bouwens et al. 2016 (re=3-14mas =17-80pc at Muv~-15) requires detailed simulations.

Future prospects with HST

Extend HFF analysis to all 6 clusters: improve the number statistics (400 galaxies at z~6; see Finkelstein talk) → more stringent limits to WDM mass.

Extend the LFL16 analysis to other redshifts (z~7-8).

Reduce the systematic effects on the Luminosity Function with state-of-the-art simulations: 1-deflection maps are more accurate than shear and deflection maps in high magnification regions; 2-size-luminosity relati

Spend 300-500 orbits on HST Cycles 25 and 26 to observe a new HFF cluster or to go deeper on existing HFF ???

MUSE deep field on HFF cluster (50 nights with Adapt-Opt): still TBD

Future prospects with JWST

JWST Deep field in (HFF?) lensing cluster pushing down to mag=30.5 (e.g. F227W, 5 sigma, 14 hours).
This corresponds to Muv=-11 at z=6. This translates into mX=4.0 keV assuming a LF of LFL16.
Assuming LF of Bouwens et al. 2016: mX=3.6 keV.
Work in progress: choose the best trade-off of filters/redshifts to optimize constraints on WDM.

Add NIRSpec+NIRISS spectroscopy to confirm the "brightest" galaxies and validate/improve the lensing model.

Synergy with other projects discussed in this meeting: Frye, Treu, Bradac, Atek, Finkelstein, Bouwens, Conselice, Suyu.

Conclusions

WDM models with spectra corresponding to thermal relic mass m_X~ 2-3 keV constitute viable solutions (models with m_X >>4 keV are indistinguishable from CDM as far as galaxy formation is concerned).

The tremendous improvement in the observations of faint galaxies at high redshift through WFC3+lensing (HFF) have allowed to measure the abundance of z=6 galaxies down to M_{UV}=-12.5 (but caveat on observational results!). This allows to set strong constraints on DM models with suppressed power spectra.

HST and JWST can be used as tools to constrain fundamental physics, i.e. the nature of Dark Matter,

independent of the modeling of astrophysical processes involving baryons!

Thank you!

Caveats

Kawamata et al. 2015
At z=6 and Muv=-21, re=1 kpc (half light radius). Assuming size-luminosity relation of Grazian et al. 2012 L^-0.5: at Muv=-12.5 re=30 pc expected, with log-normal tail at larger radii (sigma_re~60 pc).
Thus the assumption of Bouwens et al. 2016 (re=3-14mas =17-80pc at Muv~-15) requires new simulations to be confirmed.

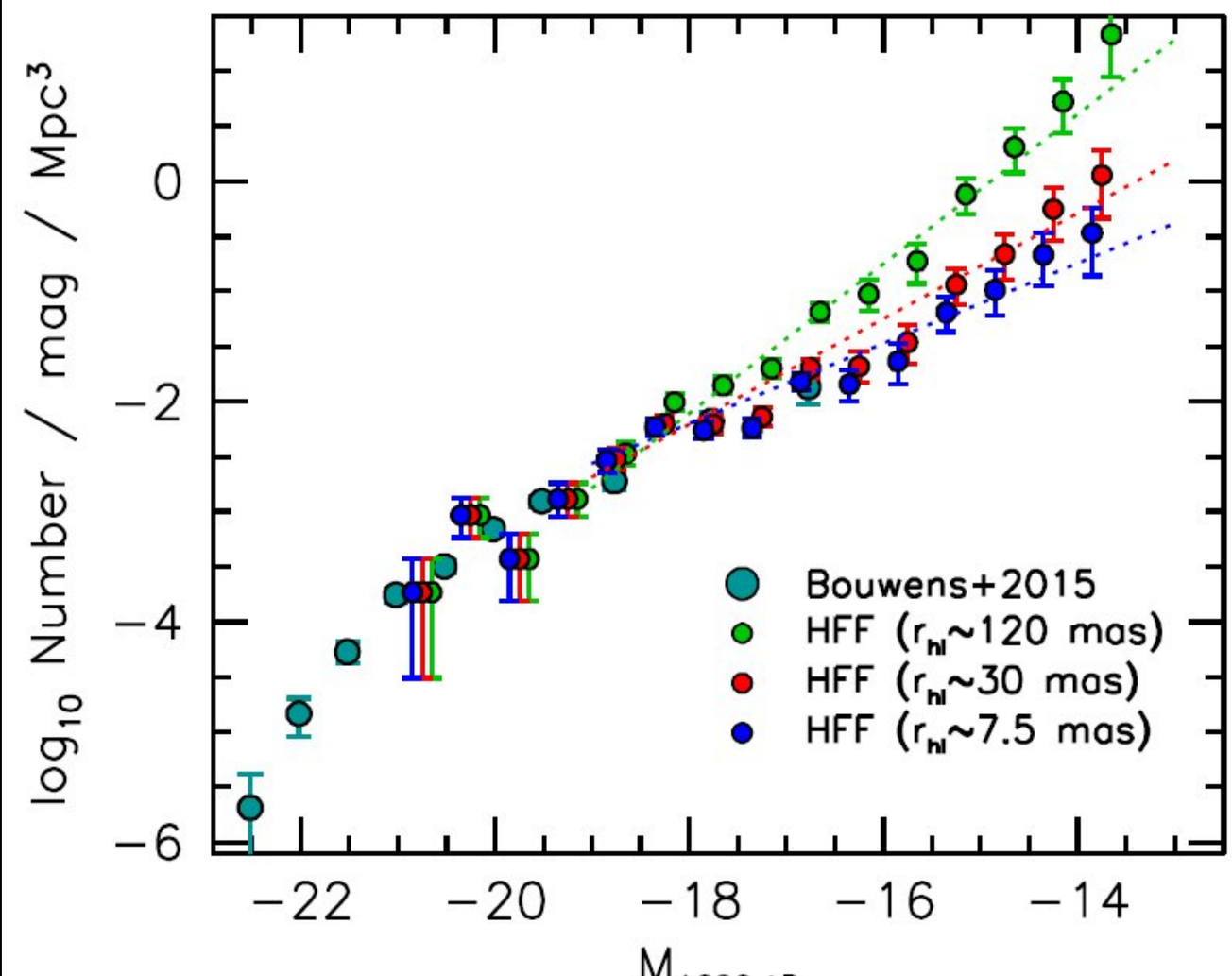

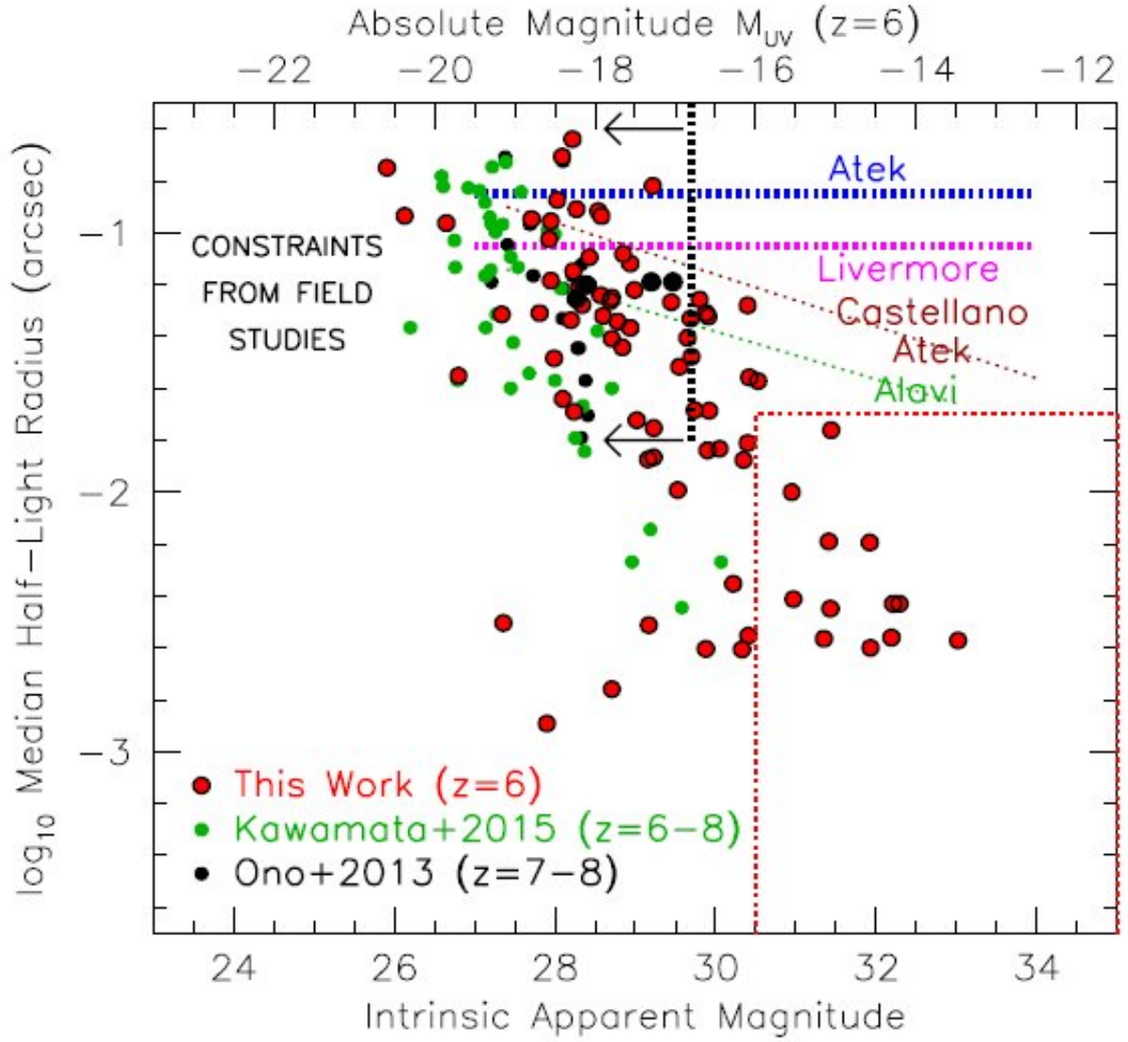

Caveats-II

Laporte et al. 2016: re=250pc at Muv=-17 at z=7.
No evolution of size fainter than Muv=-19 ???

Detailed simulations are required!!!!

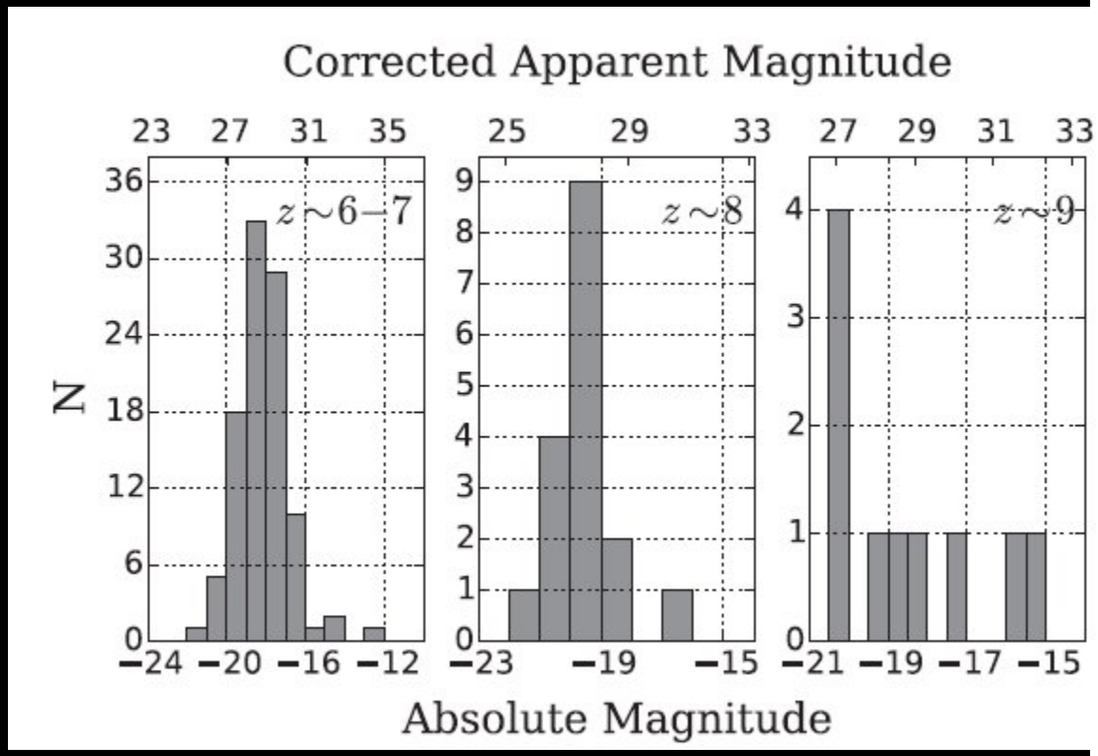

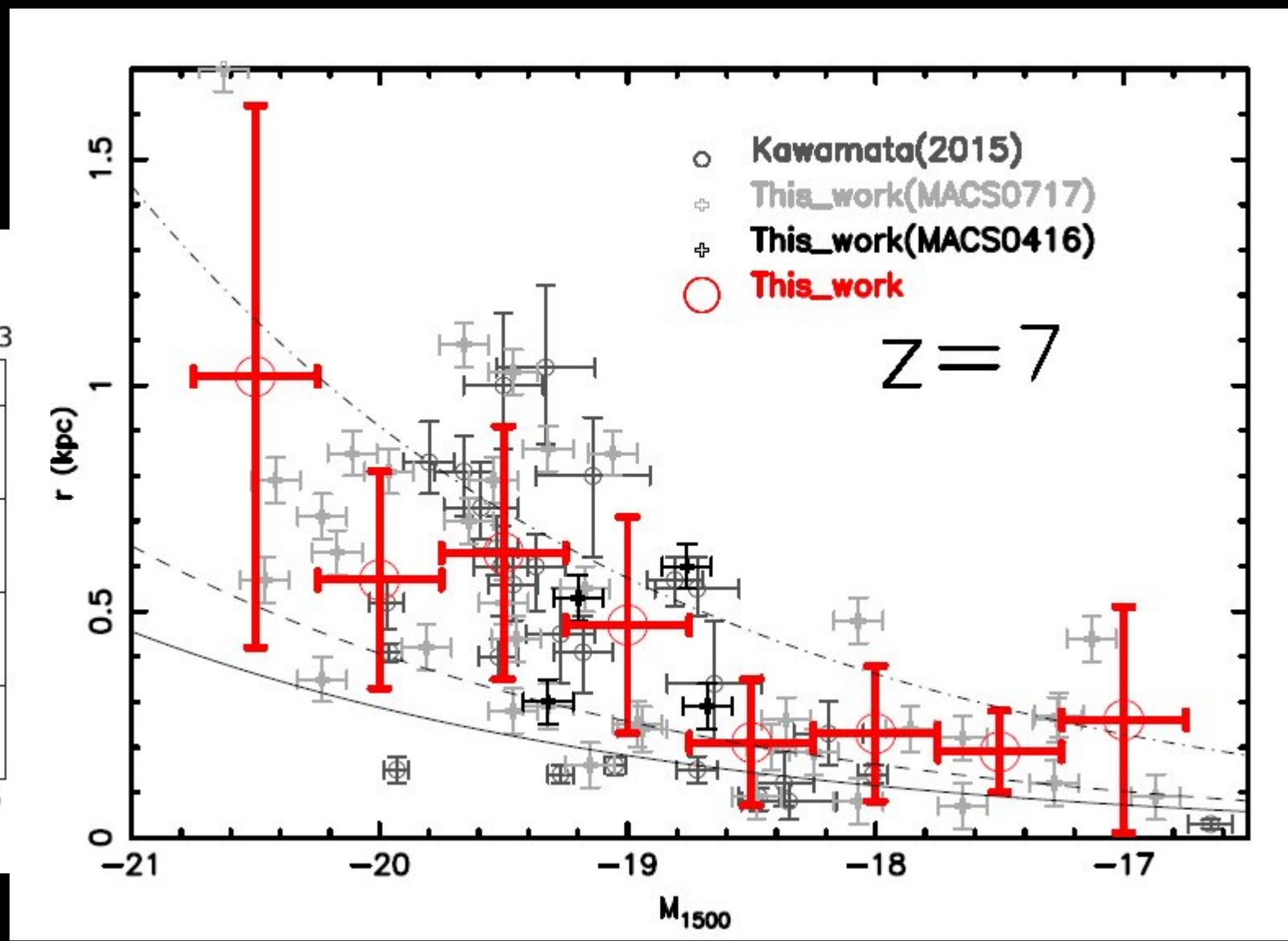

CONSTRAINING THE WDM PARTICLE MASS

In terms of thermal relic mass m_X
(conversion to sterile neutrino masses depends on production mechanism)

E.g.
Dodelson-Widrow mechanism $m_\nu \approx 2.9\ m_X$
Shi-Fuller mechanism $m_\nu \approx 2.5\ m_X$

m_X>4 keV is indistinguishable from CDM from the point of view of galaxy formation

From Thermal Relics to Sterile Neutrinos

The cutoff in the power spectrum is conventionally "labelled" according to the mass of "thermal relic" WDM particles

A similar cutoff can be achieved through WDM sterile neutrinos assuming different production mechanisms

correspondence between thermal relic mass m_X and sterile neutrino mass m_ν (yielding the same power spectrum) depends on the assumed production mechanism
E.g. for the Shi-Fuller mechanism $m_\nu \approx 2.5\, m_X$

In the following we shall show the results in terms of the equivalent thermal relic mass

Suppression with respect to CDM

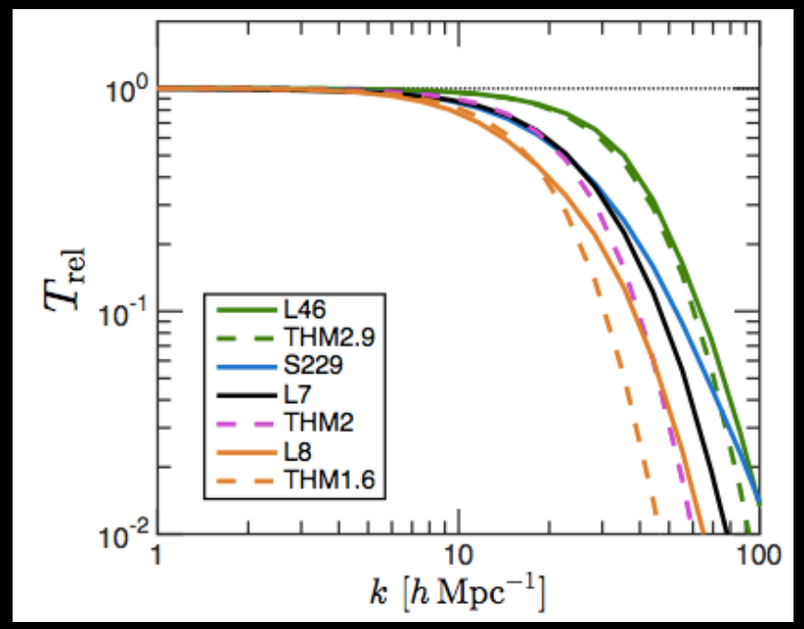

Bozek et al. 2015

Sterile Neutrinos

are produced in primordial plasma through

- off-resonance oscillations. Dodelson, Widrow; Abazajian, Fuller; Dolgov, Hansen;Asaka, Laine, Shaposhnikov et al.
- oscillations on resonance in presence of lepton asymmetry. Shi Fuller

- production mechanisms which do not involve oscillations
  – inflaton decays directly into sterile neutrinos Shaposhnikov, Tkachev
  – Higgs physics: both mass and production Petraki
  – decays of scalars in the early Universe Merle & Totzauer

From Thermal Relics to Sterile Neutrinos

The cutoff in the power spectrum is conventionally "labelled" according to the mass of "thermal relic" WDM particles

A similar cutoff can be achieved through WDM sterile neutrinos assuming different production mechanisms

correspondence between thermal relic mass m_X and sterile neutrino mass m_ν (yielding the same power spectrum) depends on the assumed production mechanism
E.g. for the Shi-Fuller mechanism $m_\nu \approx 2.5\ m_X$

In the following we shall show the results in terms of the equivalent thermal relic mass

Suppression with respect to CDM

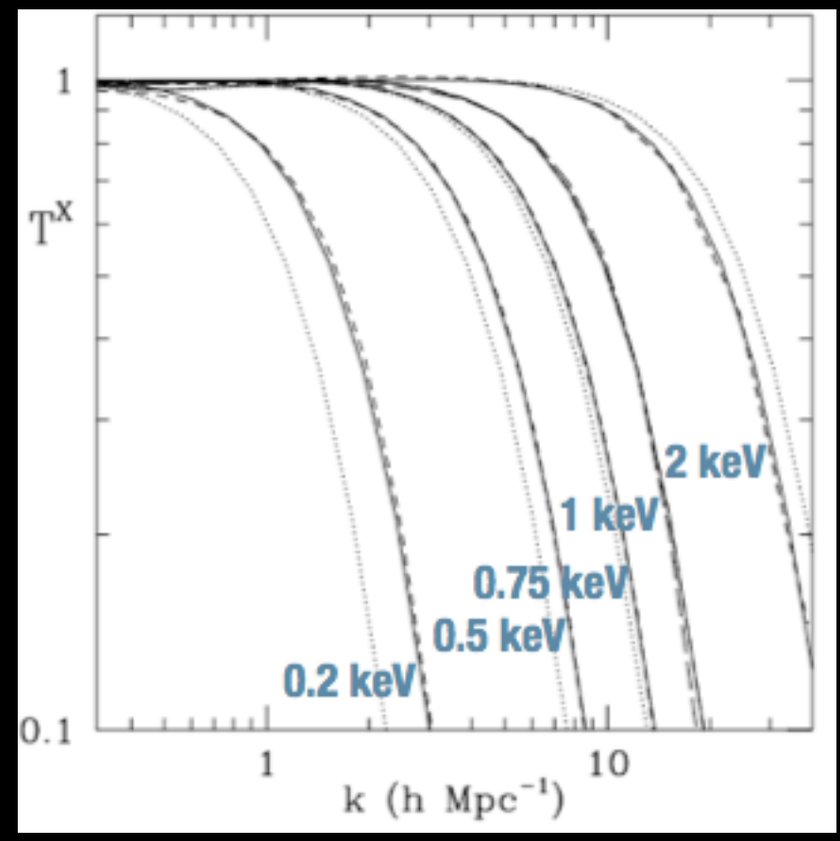

Sterile Neutrinos

if $m_s > m_\alpha$ the radiative decay $\nu_s \rightarrow \nu_\alpha + \gamma$ becomes allowed

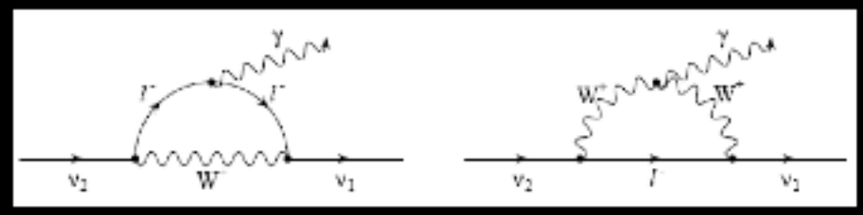

Emission lines in X-rays from DM concentrations:

- clusters (large signal but also large background)
- galaxies

$$E_\gamma = \frac{1}{2} m_s \left(1 - \frac{m_\alpha^2}{m_s^2}\right)$$

Implementing WDM power spectrum in the galaxy formation model

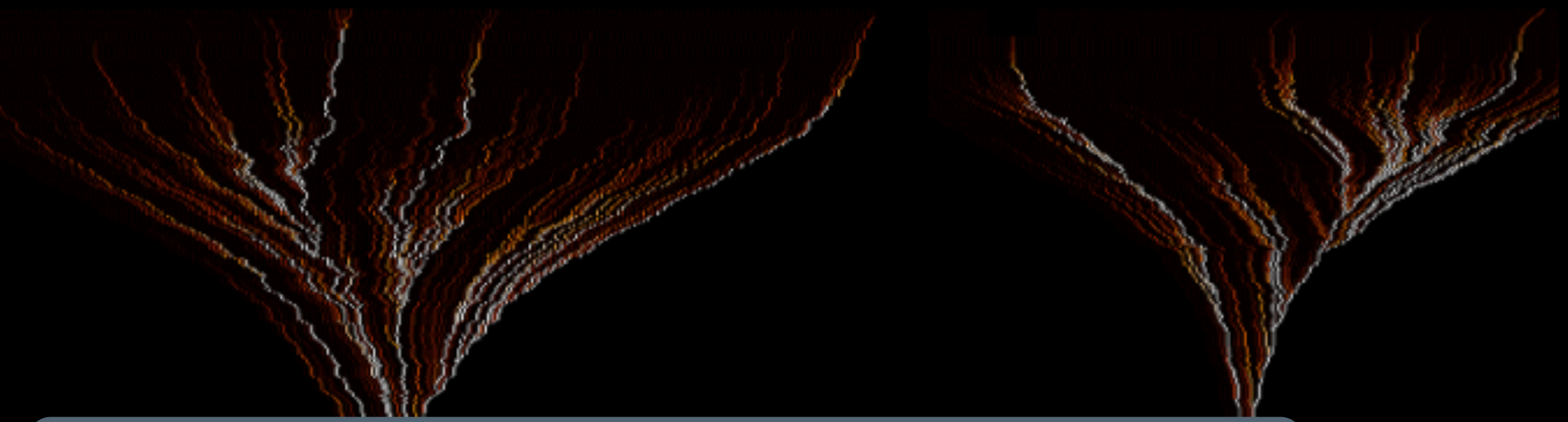

Halo Properties	Gas Properties	Star Formation	Gas Heating (feedback)	Evolution of stellar populations
Density Profiles	Profiles		SNae	
Virial Temperature	Cooling - Heating		UV background	
	Collapse			
	Disk formation			

Galaxy formation in WDM implies computing how modifications of the power spectrum propagate to the above processes

$$r_{fs} \approx 0.2 \left[\frac{\Omega_X\, h^2}{0.15}\right]^{1/3} \left[\frac{m_X}{rmkeV}\right]^{-4/3} \text{Mpc} \qquad \frac{P_{WDM}(k)}{P_{CDM}(k)} = \left[1 + (\alpha\, k)^{2\,\mu}\right]^{-5\,\mu}$$

$$\alpha = 0.049 \left[\frac{\Omega_X}{0.25}\right]^{0.11} \left[\frac{m_X}{\text{keV}}\right]^{-1.11} \left[\frac{h}{0.7}\right]^{1.22} h^{-1}\ \text{Mpc}$$

A single cluster lens provided a significant step forward

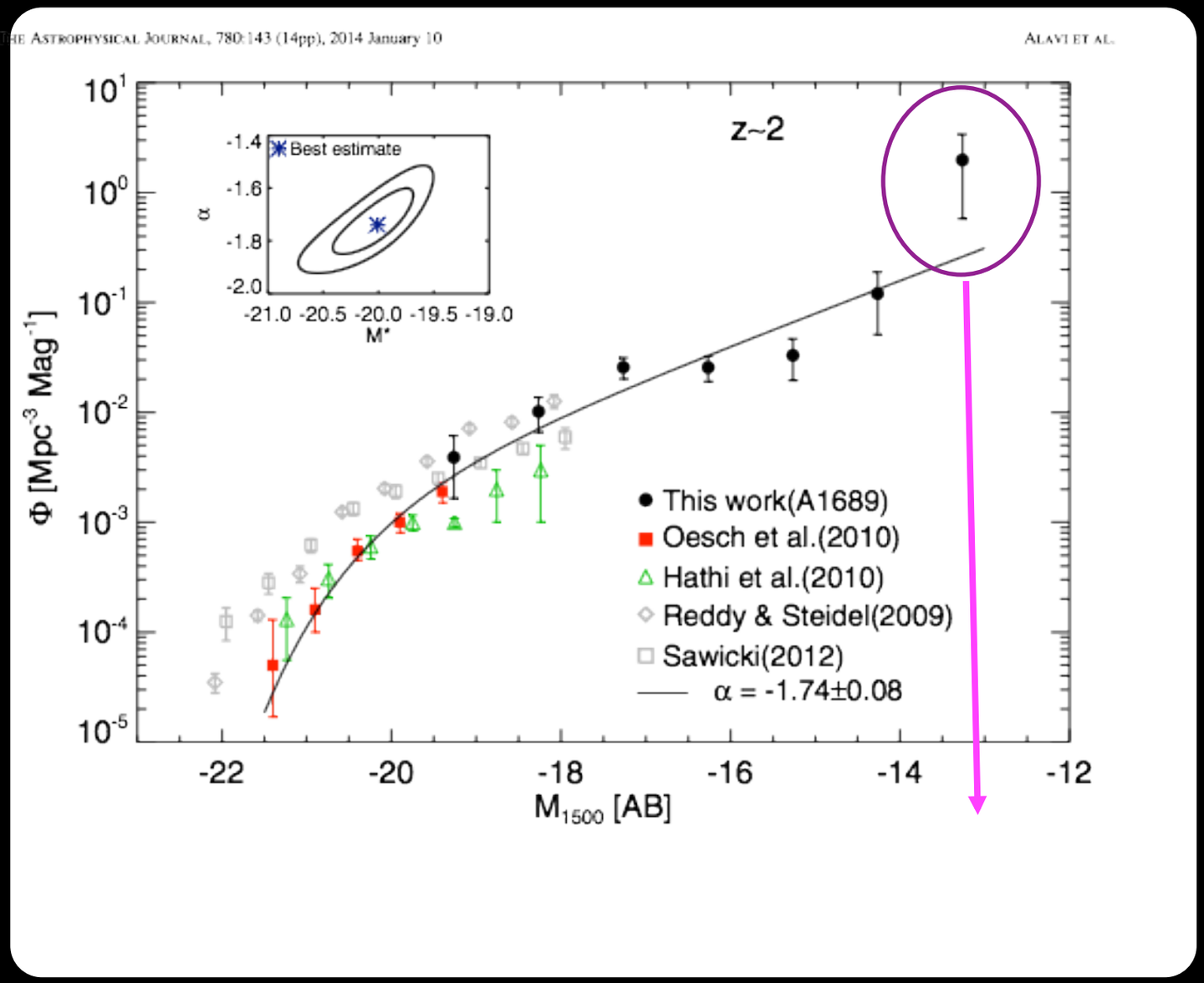

Alavi et al. 2014
Deepest Luminosity Function measured so far at z=2

Magnifications between 30 and 300

Statistics is still poor
4 galaxies in the faintest bins
$-14 \leq M_{UV} \leq -13$

Deep ultraviolet imaging of the lensing cluster A1689 with the WFC3/UVIS camera on *Hubble Space Telescope* in the F275W (30 orbits) and F336W (4 orbits) filters.
Identify z ~ 2 star-forming galaxies via their Lyman break. Because of the unprecedented depth of the images and the large magnification provided by the lensing cluster, we detect galaxies 100× fainter than previous surveys at this redshift.

A single cluster lens provided m_X>1.8 keV (thermal relic mass)

Menci, Sanchez, Grazian 2016a

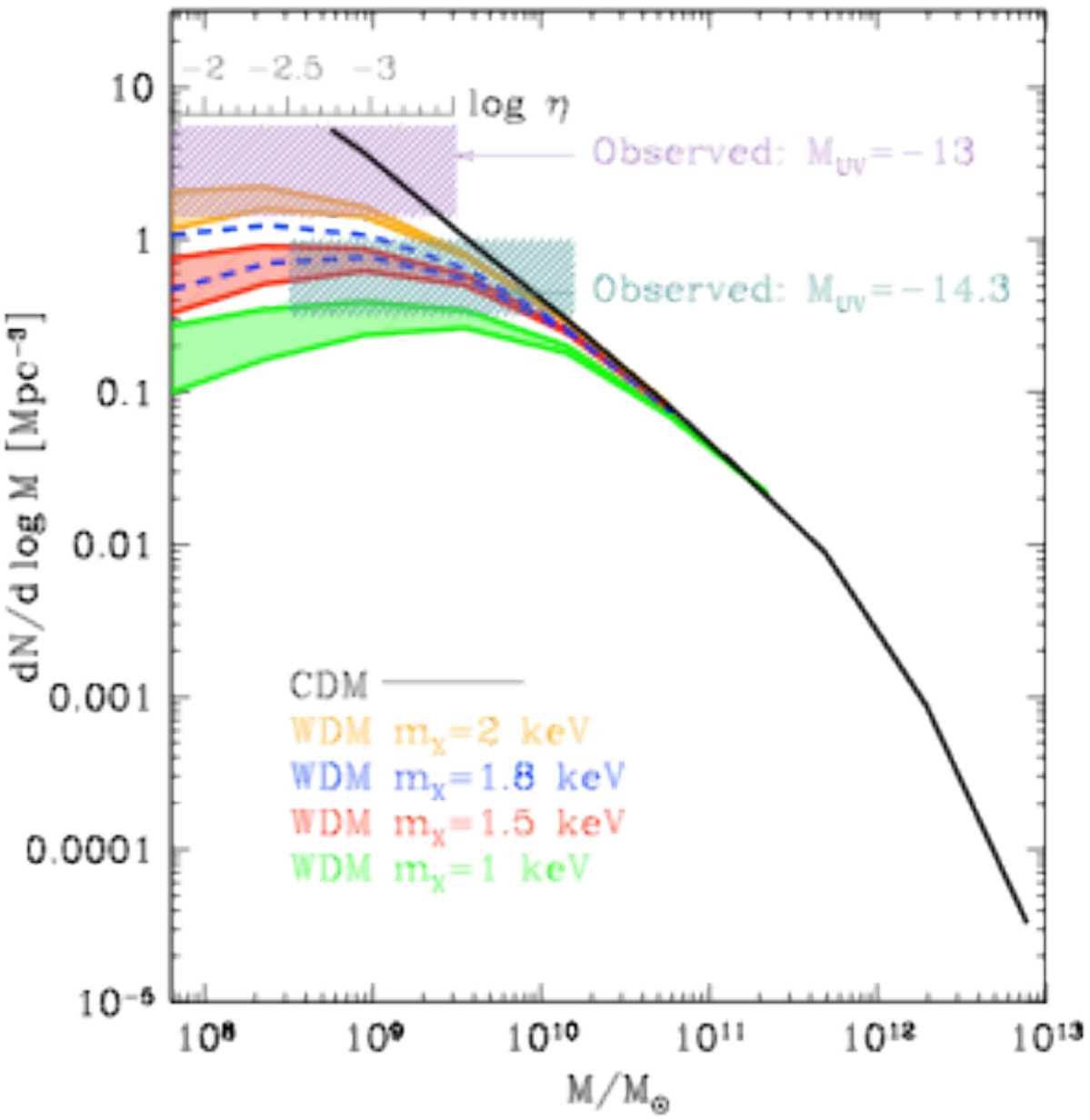

lower m_X do not provide the observed abundance. Note: baryonic processes can ma the LF flatter but not steeper !

The result is robust with respect to
The effect of baryonic processes included in η. Observations probe the mass function in the mass range around the half-mode mass where the DM mass functions are characterized by a maximum value.

The modeling of residual DM dispersion velocities. Their would yield a sharper decrease of the mass function at small masses (see, e.g., Benson et al. 2013), thus yielding tighter constraints.

The kind of DM clumps hosting the UV emitting galaxies. In fact, the upper boundaries of the solid filled regions correspond to predictions including also proto-halos.

The possible effects of UV background and reionization. Such effects would further suppress the abundance of galaxies in low-mass halos (Sawala et al. 2015).

Franse, Bulbul+16: "We examine **the flux distribution of the 3.55 keV line in the deep Suzaku observations of the Perseus cluster** in detail. **The 3.55 keV line is observed in three concentric annuli in the central observations, *although the observations of the outskirts of the cluster did not reveal such a signal***. We establish that these detections and the upper limits from the non-detections are consistent with a dark matter decay origin."

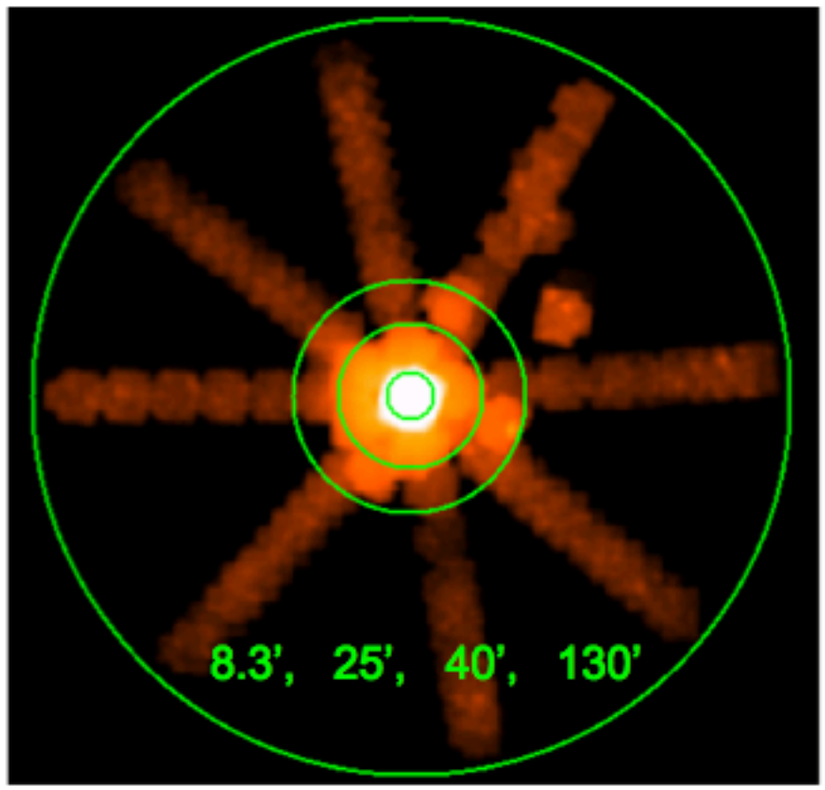

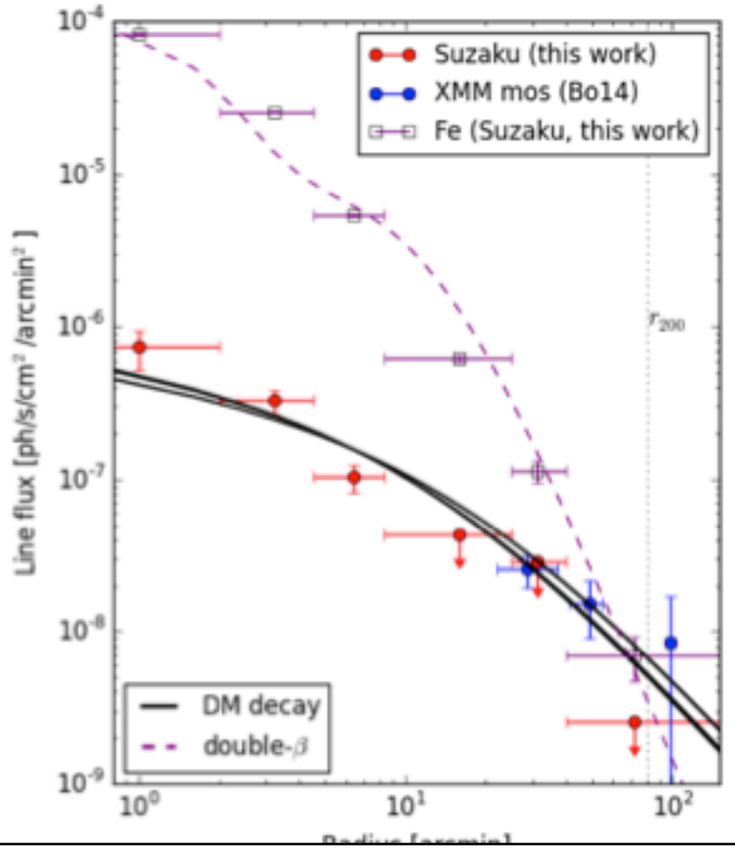

HITOMI CONSTRAINTS ON THE 3.5 KEV LINE IN PERSEUS

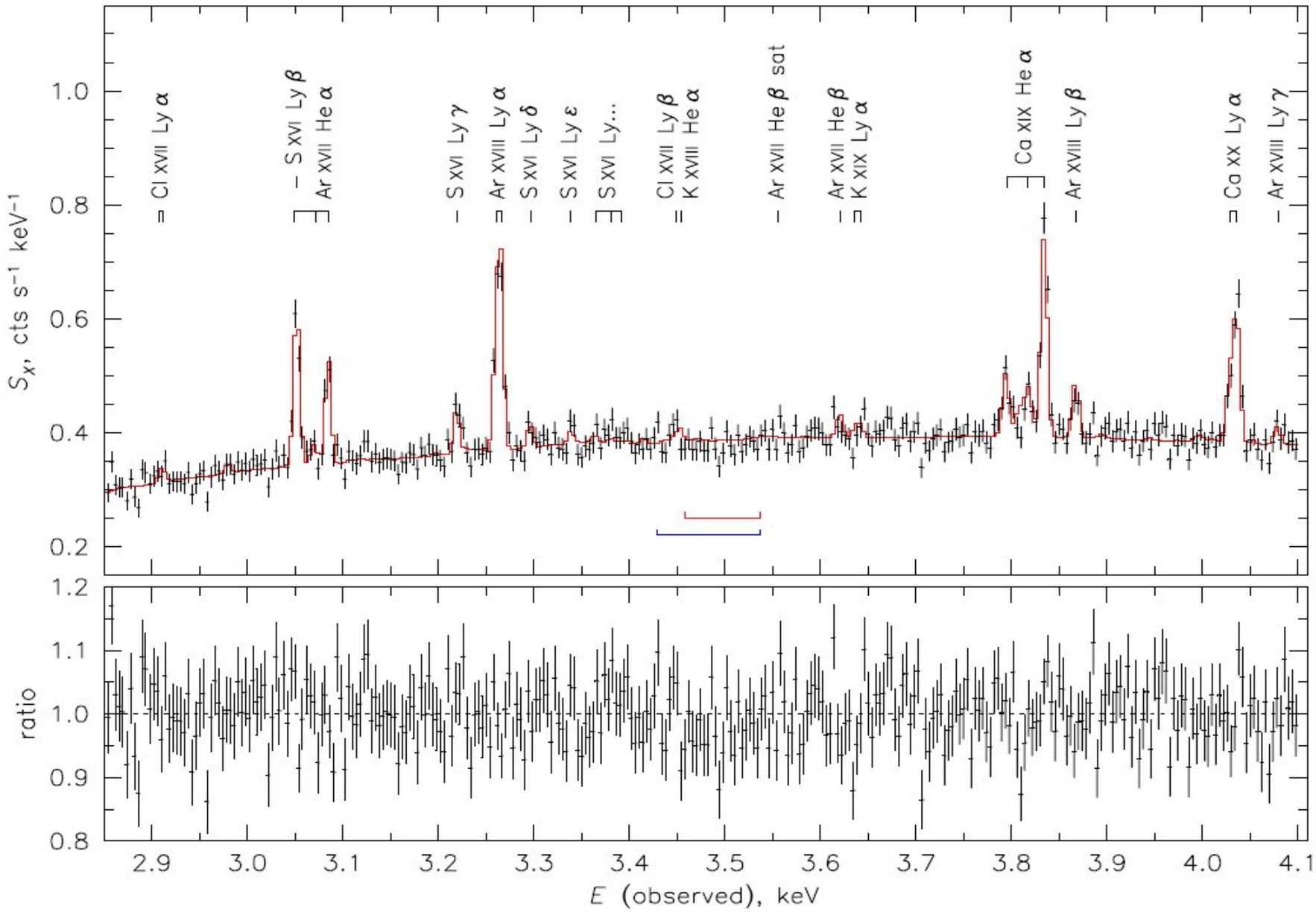

High-resolution X-ray spectroscopy with *Hitomi* was expected to resolve the origin of the faint unidentified $E \approx 3.5$ keV emission line reported in several low-resolution studies of various massive systems, such as galaxies and clusters, including the Perseus cluster. We have analyzed the *Hitomi* first-light observation of the Perseus cluster. The emission line expected for Perseus based on the *XMM-Newton* signal from the large cluster sample under the dark matter decay scenario is too faint to be detectable in the *Hitomi* data. However, the previously reported 3.5 keV flux from Perseus was anomalously high compared to the sample-based prediction. We find no unidentified line at the reported flux level. The high flux derived with *XMM* MOS for the Perseus region covered by *Hitomi* is excluded at $> 3\sigma$ within the energy confidence interval of the most constraining previous study. If *XMM* measurement uncertainties for this region are included, the inconsistency with *Hitomi* is at a 99% significance for a broad dark-matter line and at 99.7% for a narrow line from the gas. We do find a hint of a broad excess near the energies of high-n transitions of S XVI ($E \simeq 3.44$ keV rest-frame) — a possible signature of charge exchange in the molecular nebula and one of the proposed explanations for the 3.5 keV line. While its energy is consistent with *XMM* pn detections, it is unlikely to explain the MOS signal. A confirmation of this interesting feature has to wait for a more sensitive observation with a future calorimeter experiment.

Subject headings: Dark matter — galaxies: clusters: individual (A426) — galaxies: clusters: intracluster

Non-Thermal Relics: Resonant Production of sterile neutrinos (Shi Fuller 1999)

NM, Merle Schneider, Toutzer, Sanchez Cstellano, Grazian in progress

Off resonance with negligible lepton asymmetry: Dodelson Widrow scenario: mixing angles too large (conflicts with bounds from X-ray observations)

Sterile neutrinos could be produced from neutrino oscillations: for a
a given lepton asymmetry, oscillations on Mikheev–Smirnov–Wolfenstein (MSW) resonance generate a greater abundance of relic sterile neutrinos with a lower average momentum than in the DW case.

Lepton asymmetry related to mixing angle to reproduce observed DM density

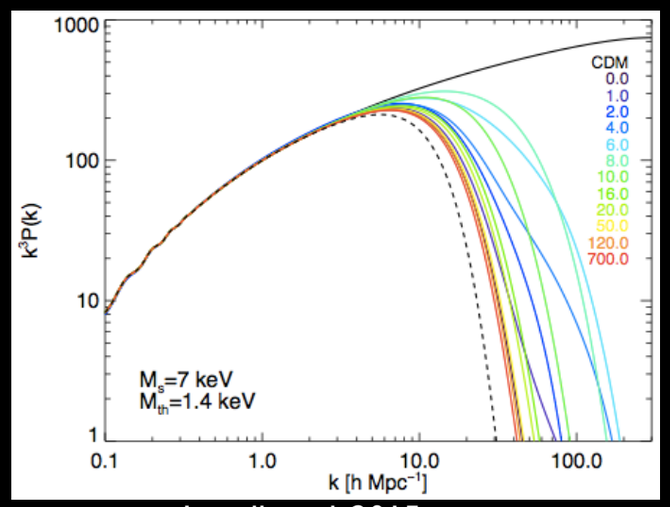

Lovell et al. 2015

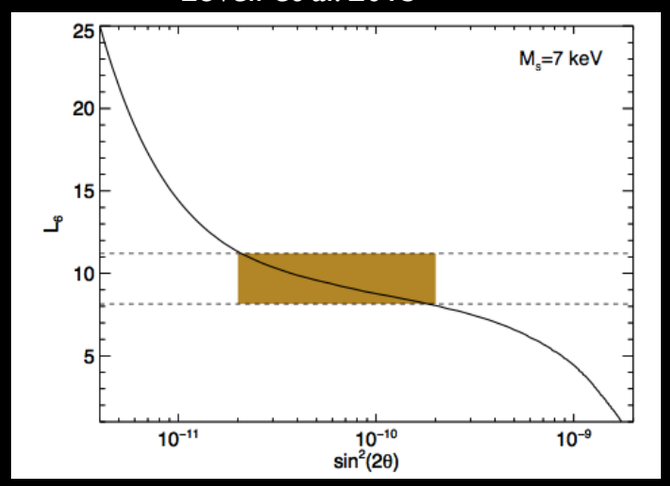

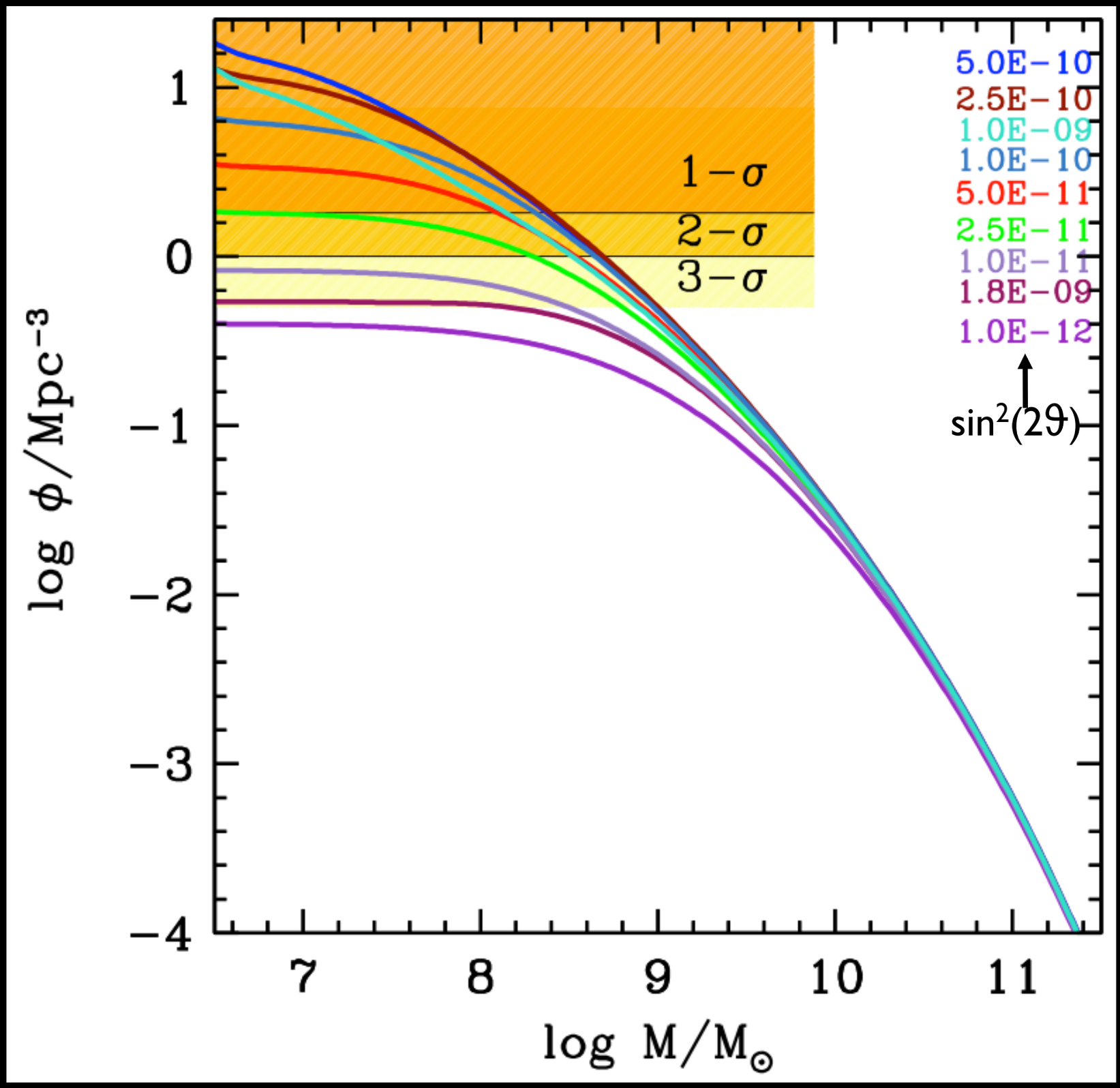

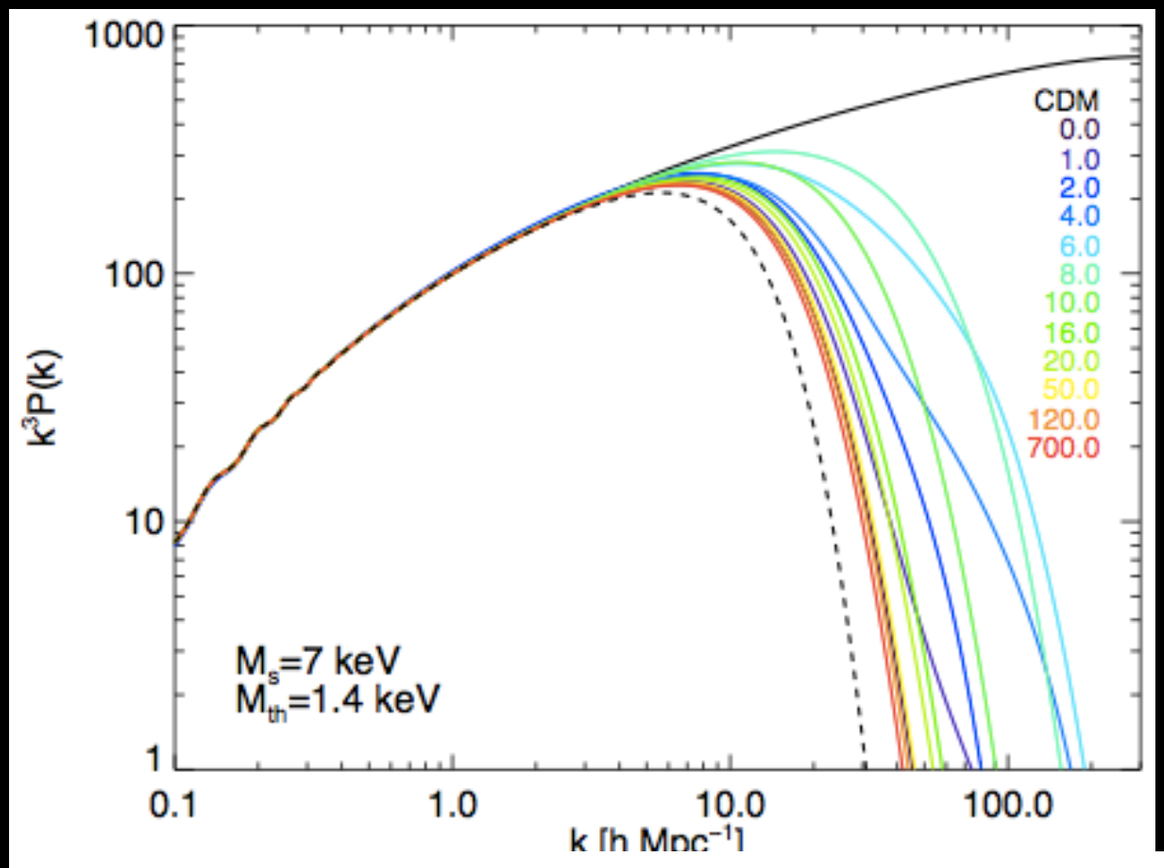

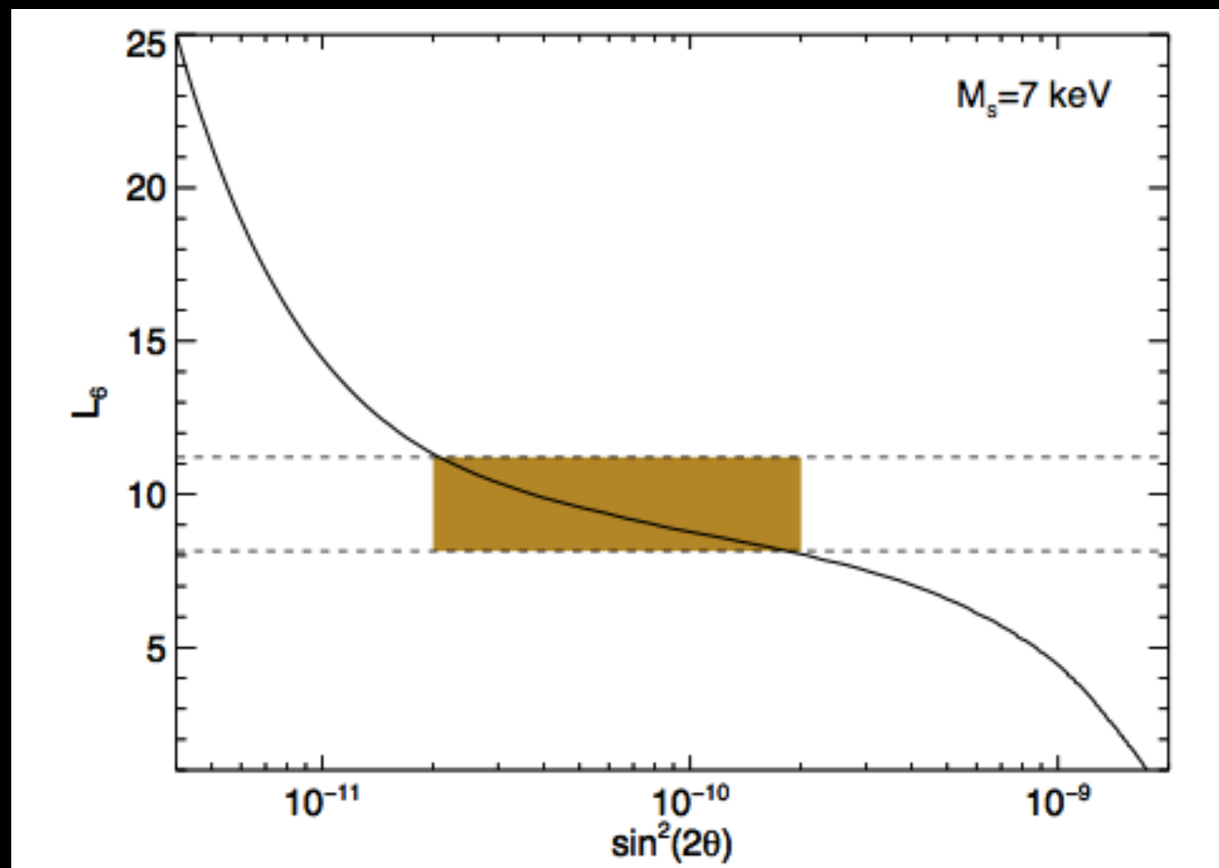

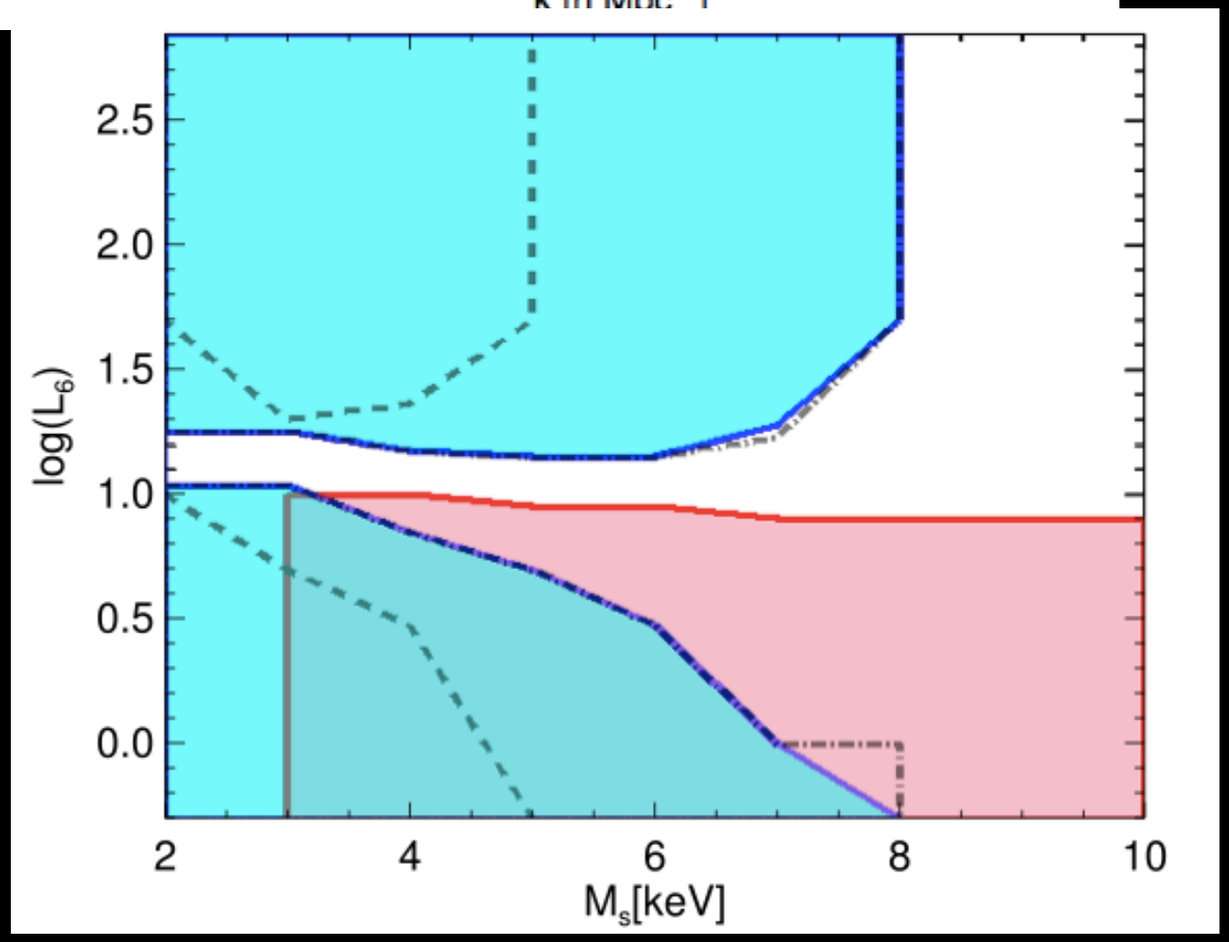

8 0 -12

8 50 -12

7 15 -11

6 12 5e-11

5 12 1-10

4 15 -11

3 15 -11

Resonant Production of sterile neutrinos: constraints on the $\sin^2(2\vartheta)$-$m_{sterile}$ plane

X-ray Bounds

$$\Gamma_{\nu_s \to \gamma\nu} \simeq 1.38 \times 10^{-22} \sin^2 2\theta \left(\frac{m_{\rm sn}}{\rm keV}\right)^5 \ s^{-1}$$

$$F_\gamma = \frac{\Gamma_{\nu_s \to \gamma\nu}\, \Omega_{\rm fov}}{8\pi} \int_{\rm los} dx\, \rho_{\rm DM}(x)$$

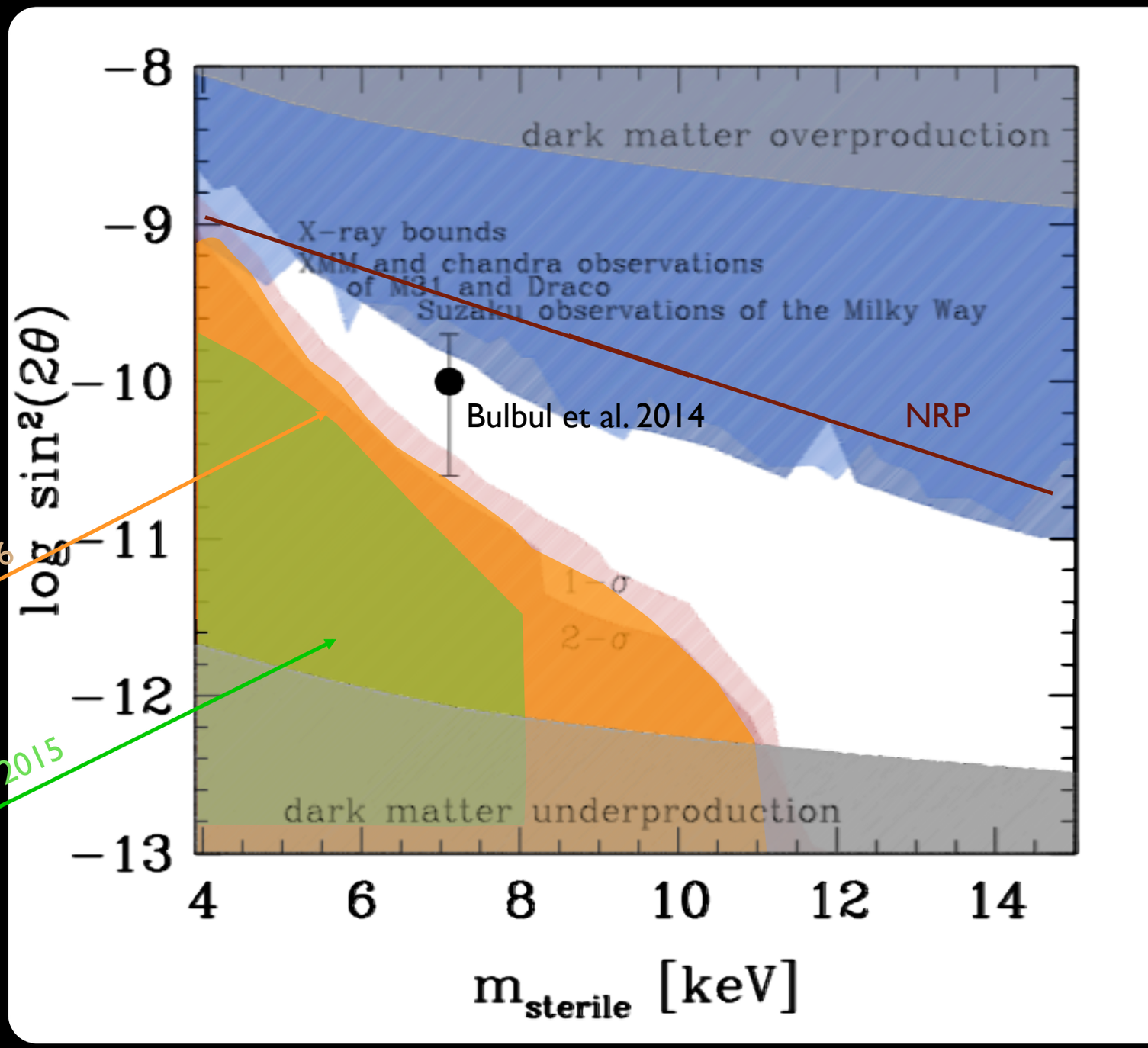

Limits from Milky Way satellites: depend on

- assumed upper limit for MW mass
- assumed lower limit for satellite masses
- assumed isotropic distribution to correct SDSS observations for limited sky coverage
- assumed halo-to-halo variance

Sterile neutrinos from scalar decay (Merle et al. 2013)

Scalar field S coupled to the right-handed neutrino fields N. The most generic coupling is a Yukawa term with coupling strength y which, if the scalar develops a non-zero vacuum expectation value ⟨S⟩, leads to a Majorana mass $m_N = y\langle S\rangle$. IF $\langle S\rangle \approx$ GeV − TeV → y ~ 10^{-9}–10^{-5} in order for the mass of the sterile neutrino to be in the keV-range.

y determines the decay time of the scalar.

For a given sterile neutrino mass, matching the observed DM density leaves y as the only free parameter
(for small Higgs portal coupling $\lambda \ll 10^{-6}$).

$y>10^{-8}$ at 2-σ level for $m_{sterile}$=7 keV

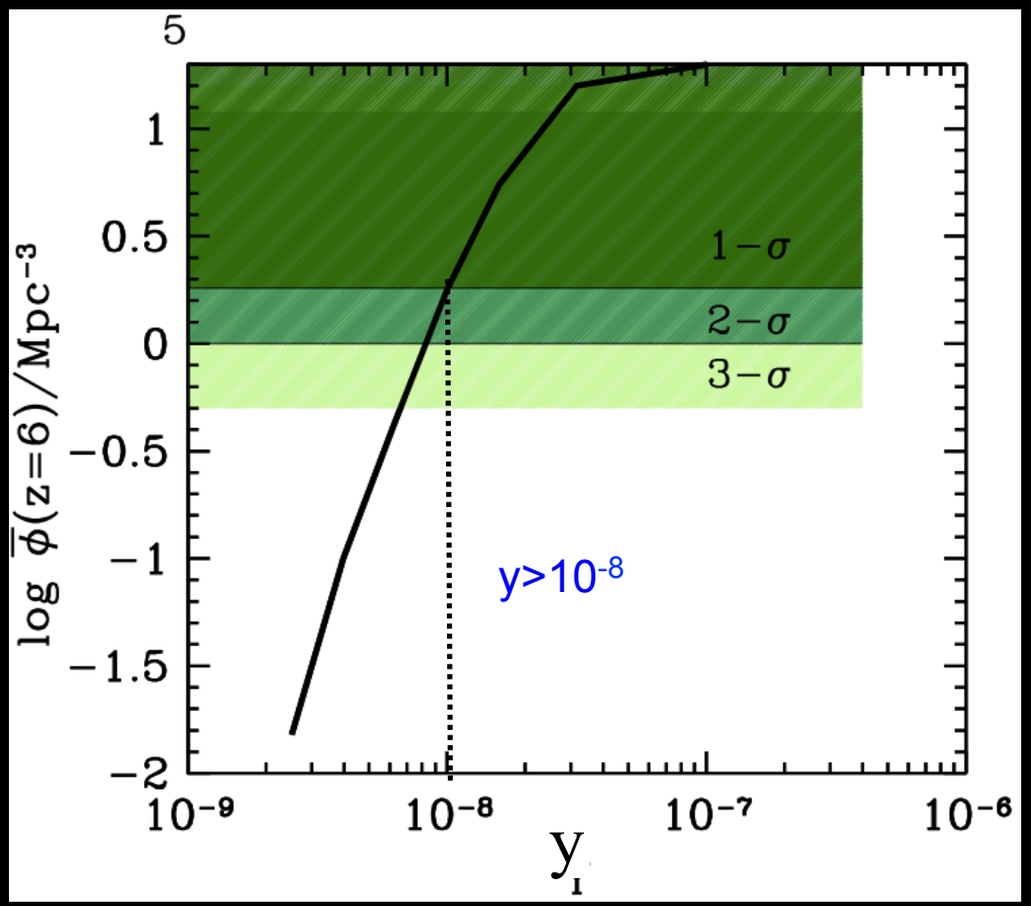

NM, Merle Schneider, Toutzer, Sanchez Cstellano, Grazian 2016

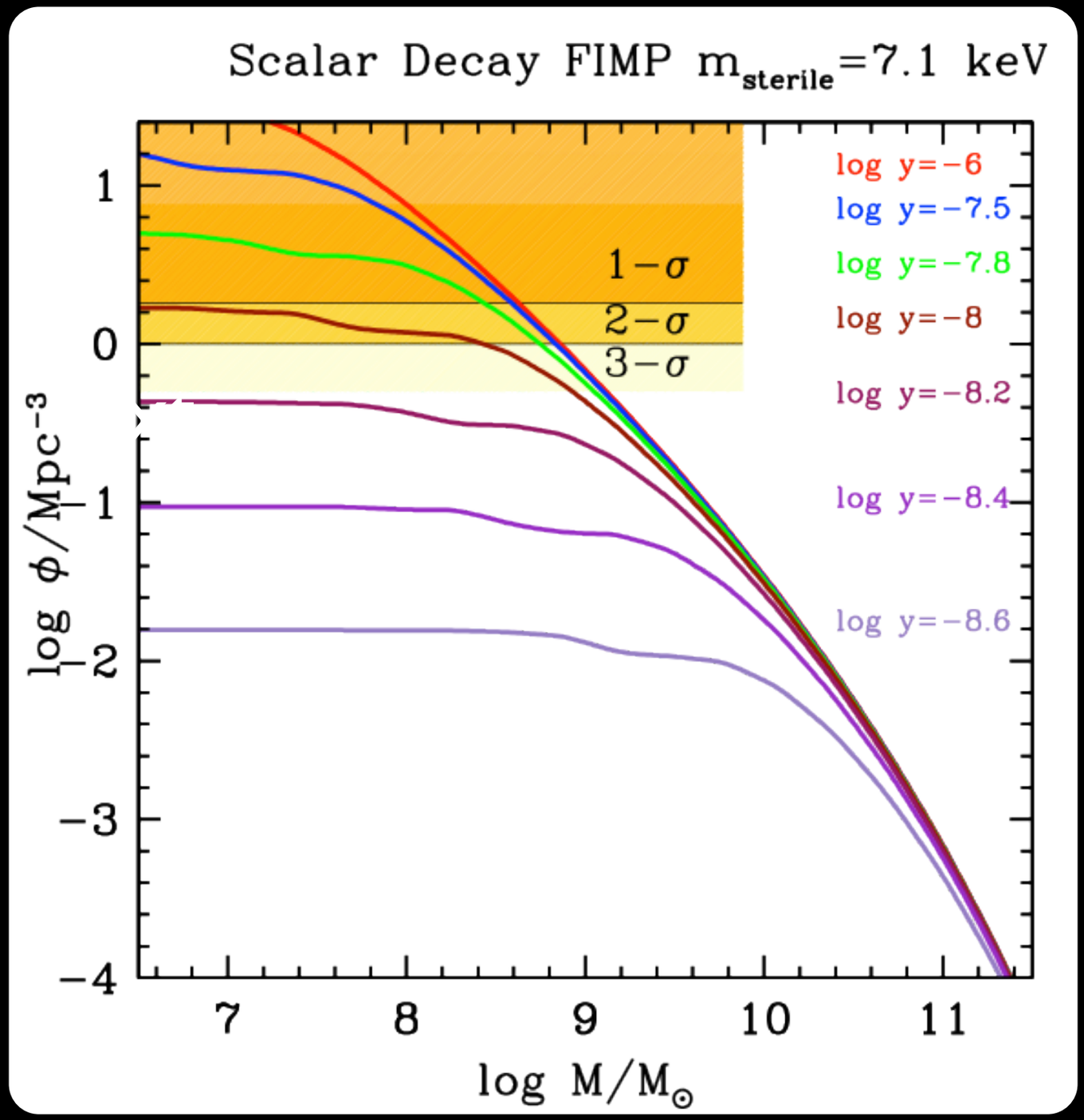

The ultra-deep LF at z=6 constitute an extremely powerful probe

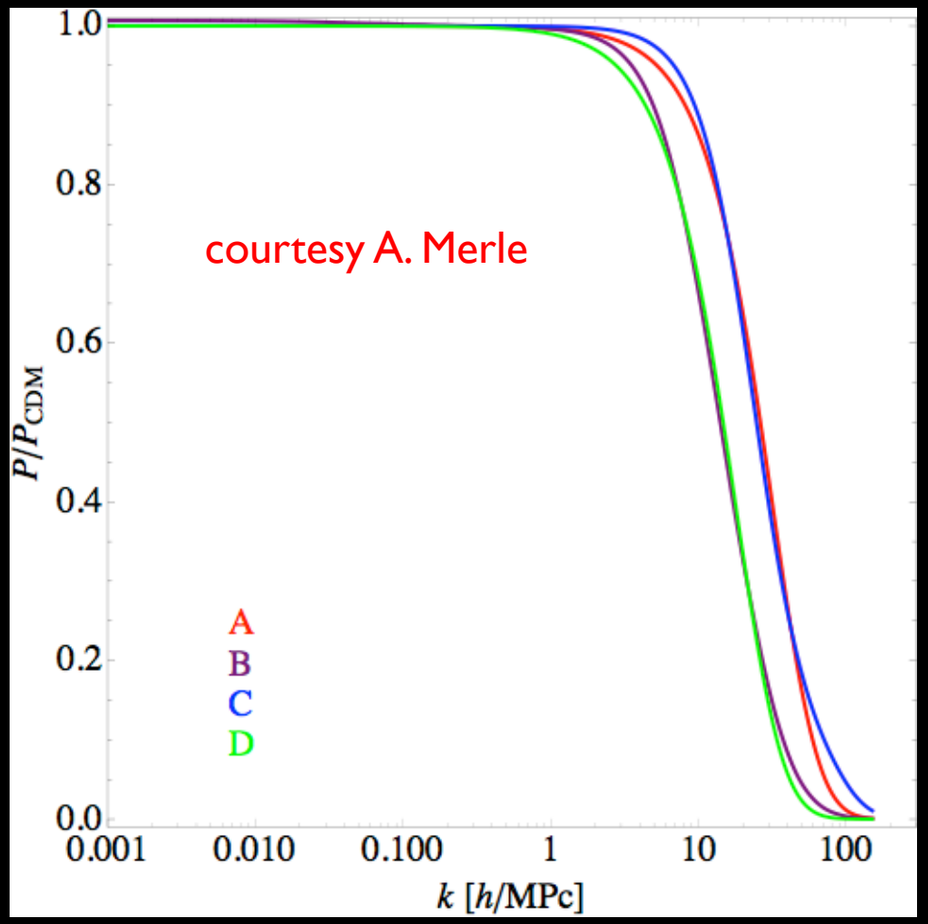

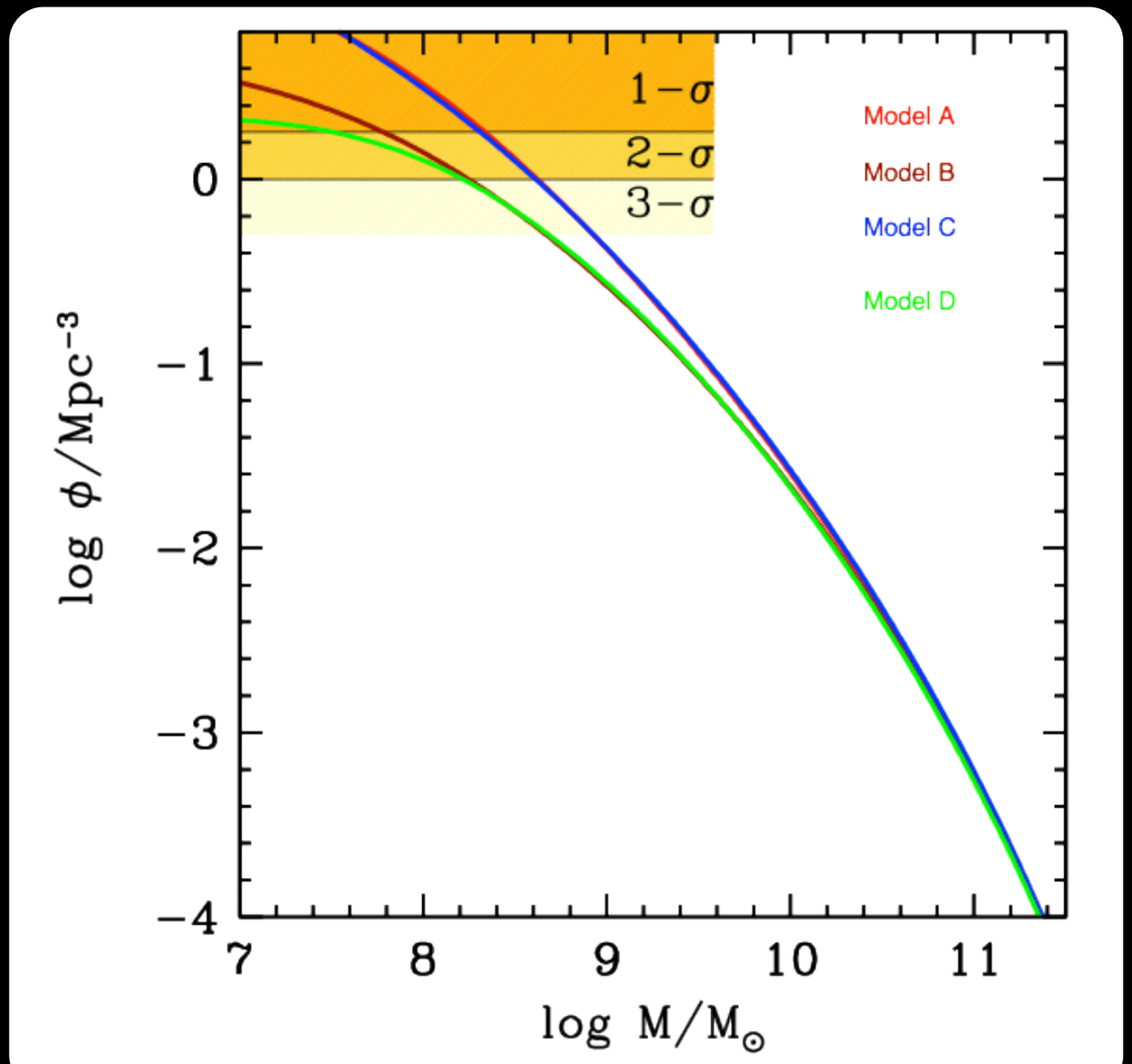

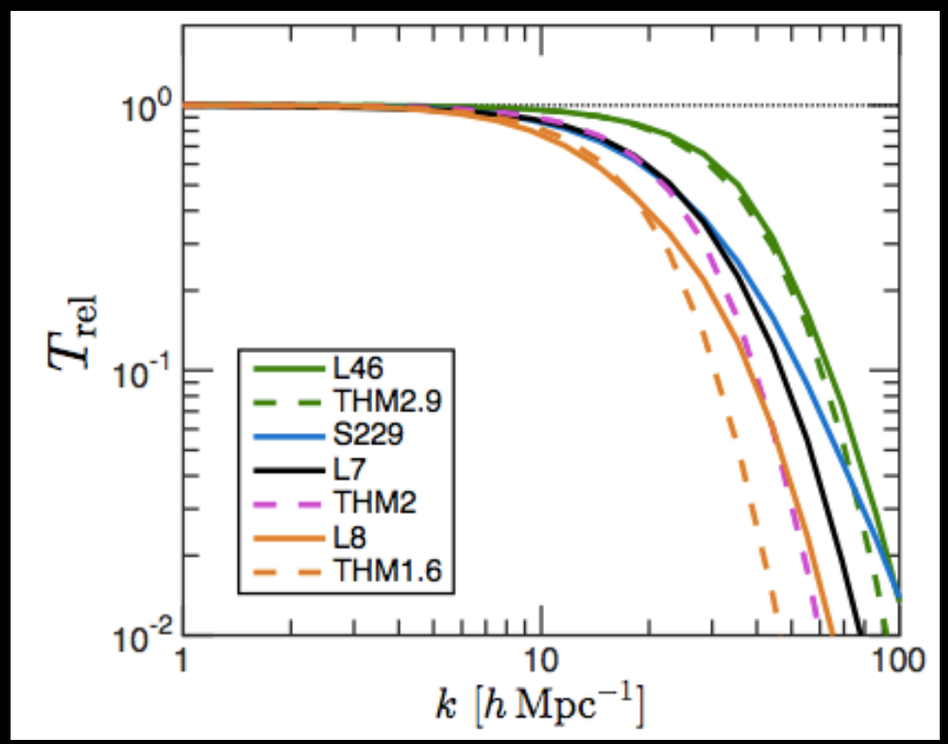

Bozek et al. 2015

Wave DM - Fuzzy Dm: Bose condensate of ultra-light axion $m_X \sim 10^{-22}$ ev.

wavelike dark matter composed of a non-relativistic Bose-Einstein condensate,
so the uncertainty principle counters gravity below a Jeans scale (see Hu et al. 2000)

coulping Schrodinger's equation to gravity via Poisson's equation: a new form of stress tensor from quantum uncertainty, giving rise to a comoving Jeans length $\lambda_J \propto (1 + z)^{1/4} m_B^{-1/2}$
A distinct gravitationally self-bound solitonic core is found at the center of every halo, with a profile quite different from cores modeled in the warm or self-interacting dark matter scenarios.

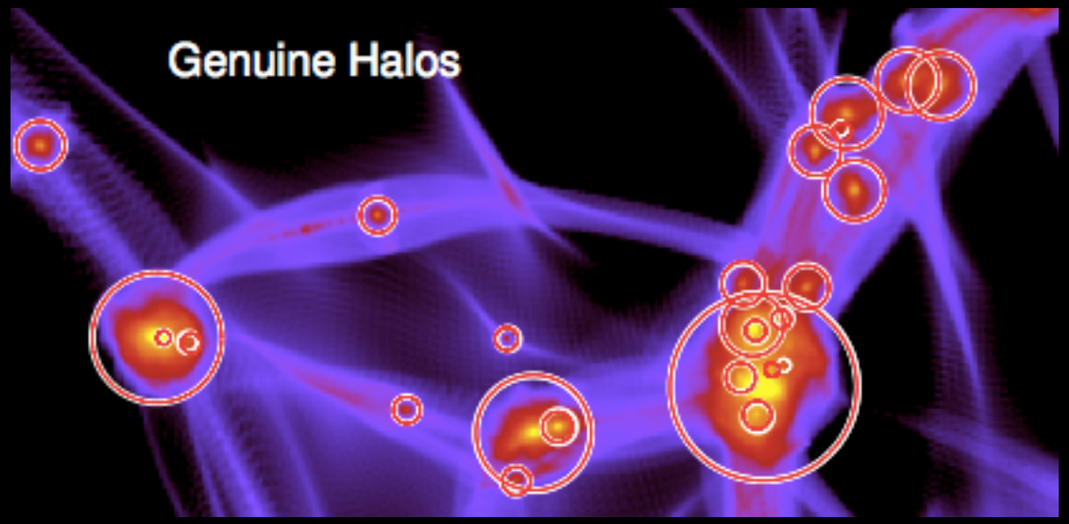

Schive, Chiueh, Broadhurst 2014

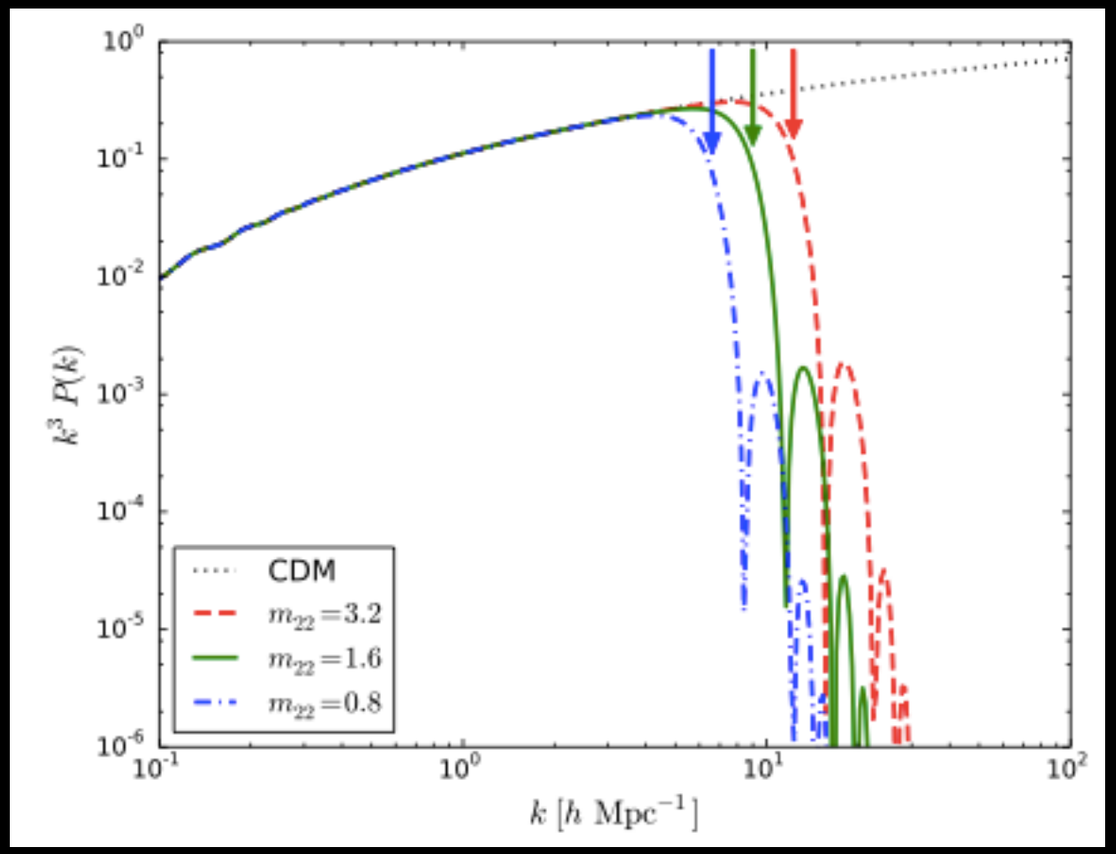

Wave DM - Fuzzy Dm: Bose condensate of ultra-light axion $m_X \sim 10^{-22}$ ev.
Such class of models is ruled out

matching observed abundance of z=6 galaxies requires $m_{22}>10$
Matching the dwarf profiles requires $m_{22}<1.2$

Schive et al. 2016

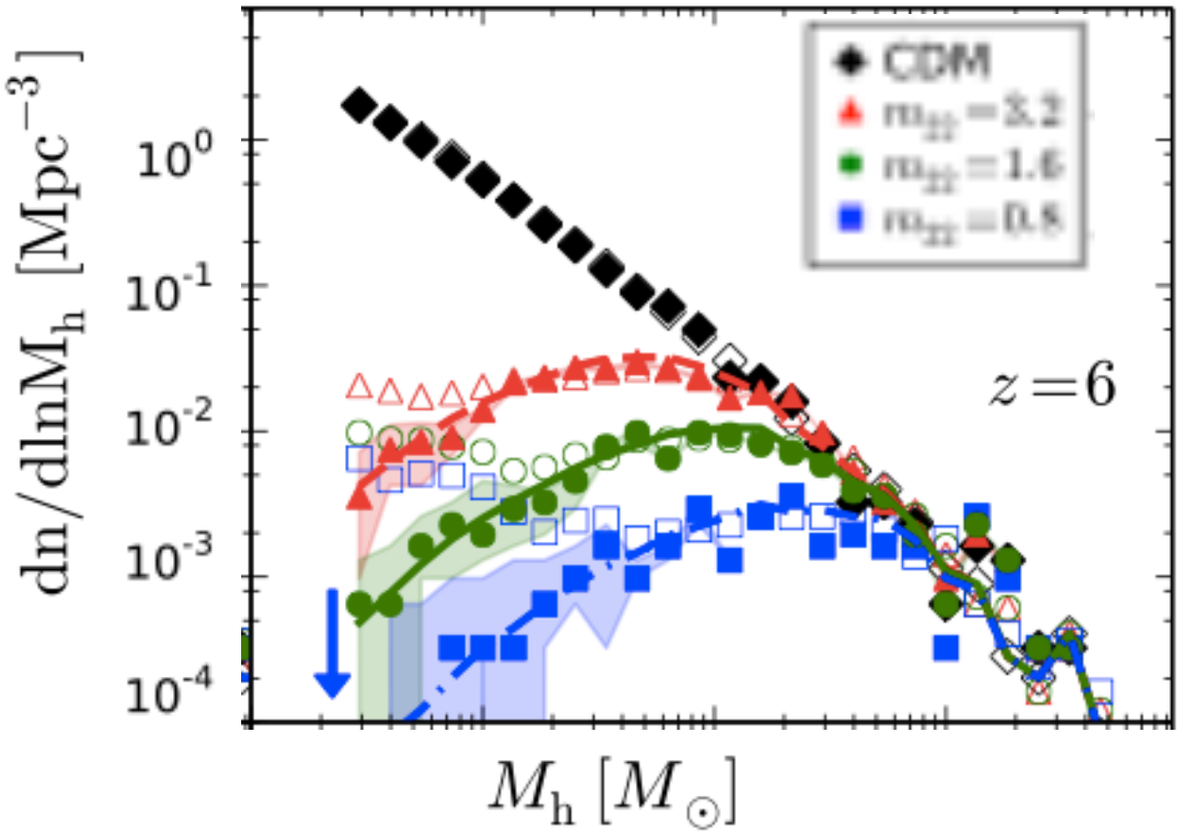

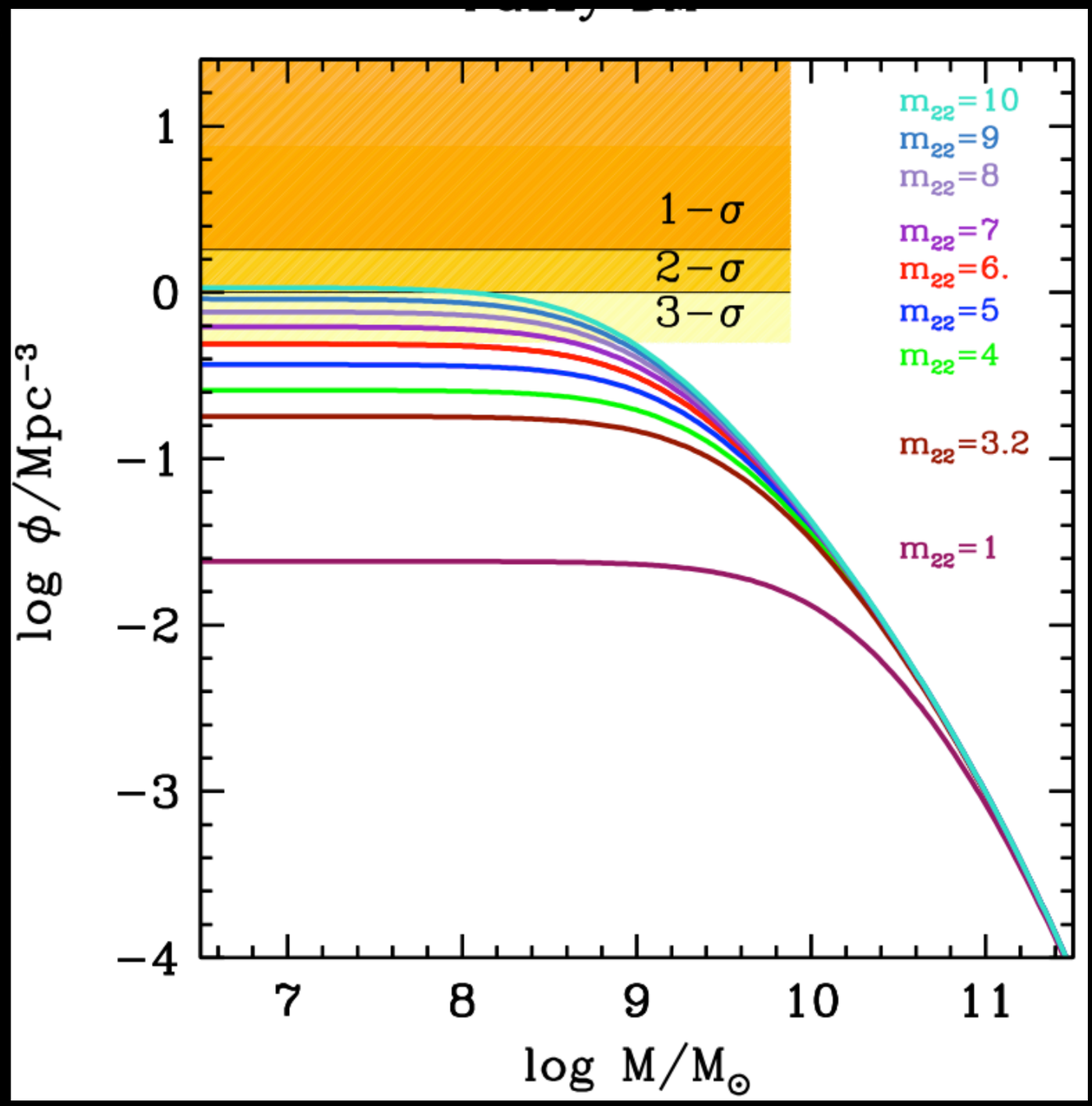

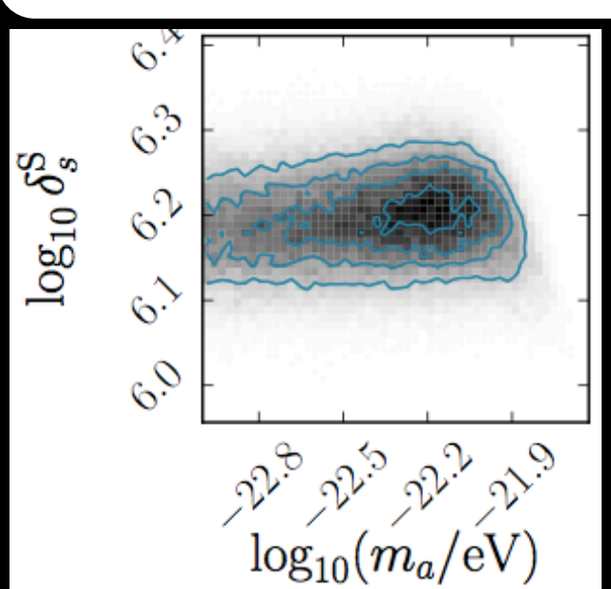

Marsch et al. 2015

Cosmic Structures form from the collapse of overdense regions in the DM primordial density field, and grow by gravitational instability

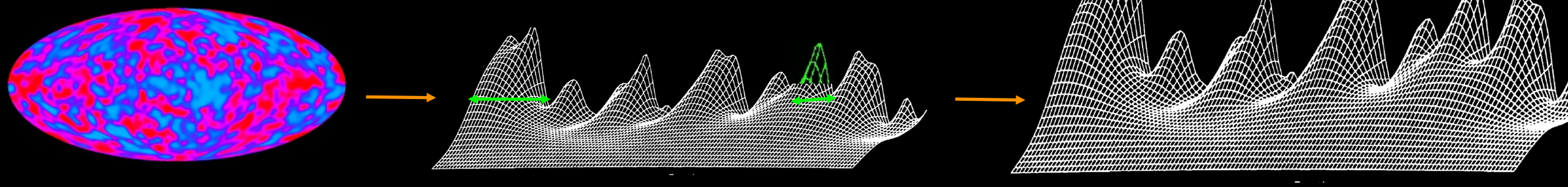

$R = 2\pi/k$

$$M = \frac{4\pi}{3} \rho R^3$$

$$\langle \delta_M^2 \rangle = \sigma^2(M)\, g(t)$$

Gaussian Random field

$$\delta = \frac{\delta\rho}{\rho}$$

$$p(\delta_k) = \frac{1}{\sqrt{2\pi}\,\sigma_k} e^{-\frac{\delta_k^2}{2\,\sigma_k^2}}$$

Mean (square) value of perturbations of size R(~1/k) enclosing a mass M

$$P(k) = \frac{1}{V} \langle |\delta_k|^2 \rangle$$

$$\sigma_M^2 = \frac{1}{(2\pi)^3\, V} \int^{M \leftrightarrow k} dk\, k^2\, P(k)$$

$$\sigma_M^2 \leftrightarrow P(k)$$

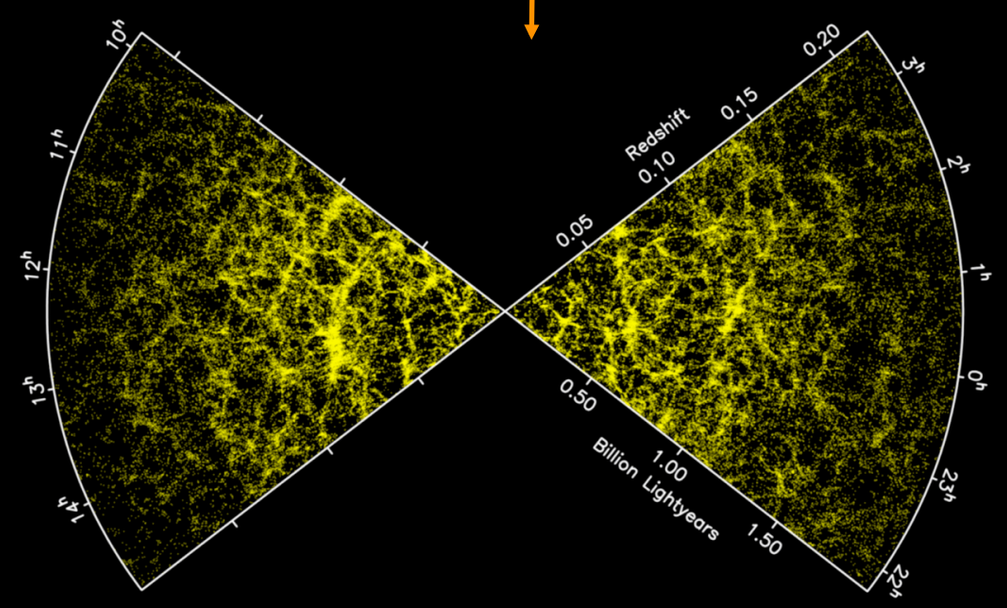

Variance σ (M) quantifies the typical amplitude of density perturbations on a given mass scale

The Variance of the perturbation field

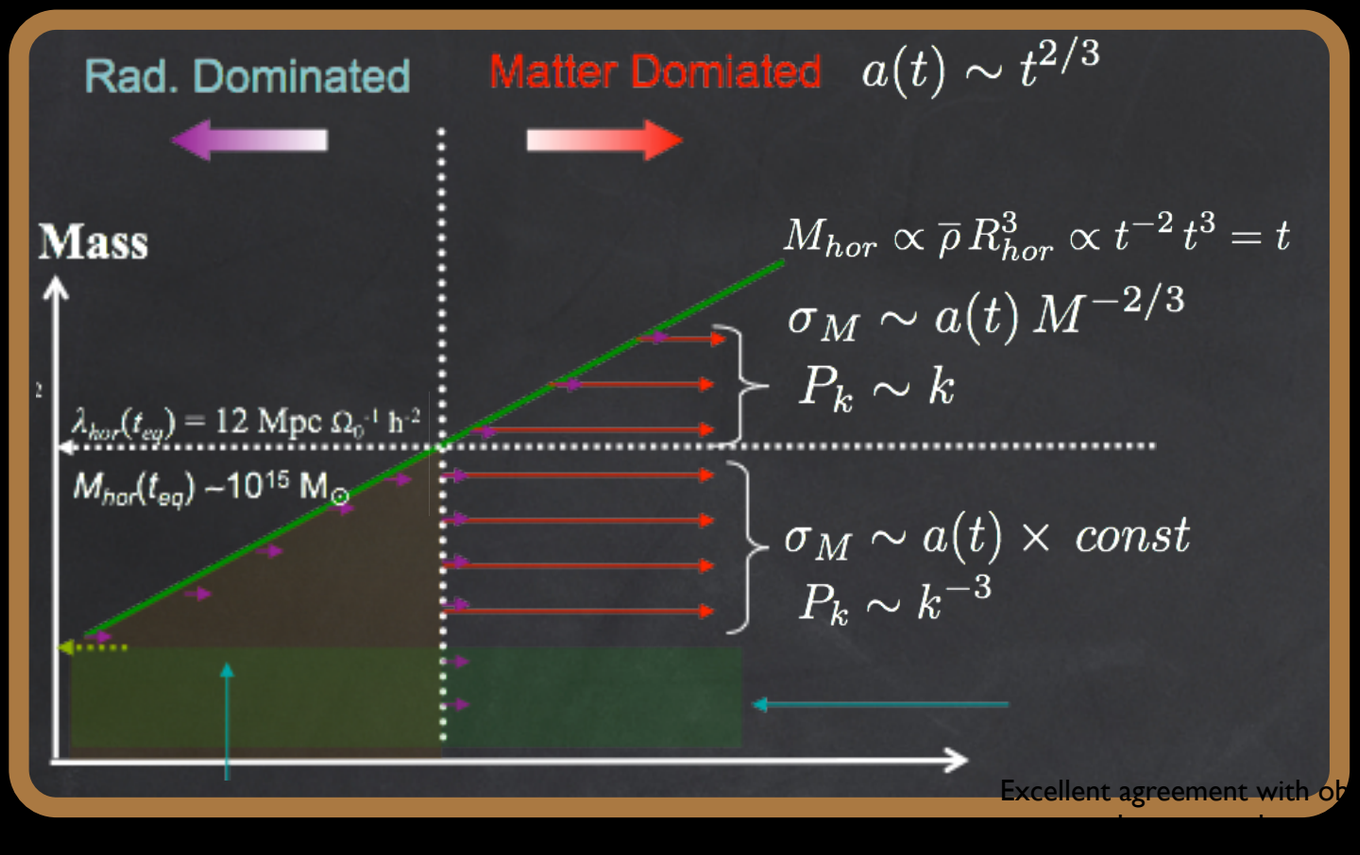

Cold Dark Matter

non relativistic at decoupling

no dissipation down to small scales < 10^6 M$_\odot$

Variance is an ever-increasing inverse function of the mass scale.

Huge number of small-scale structures

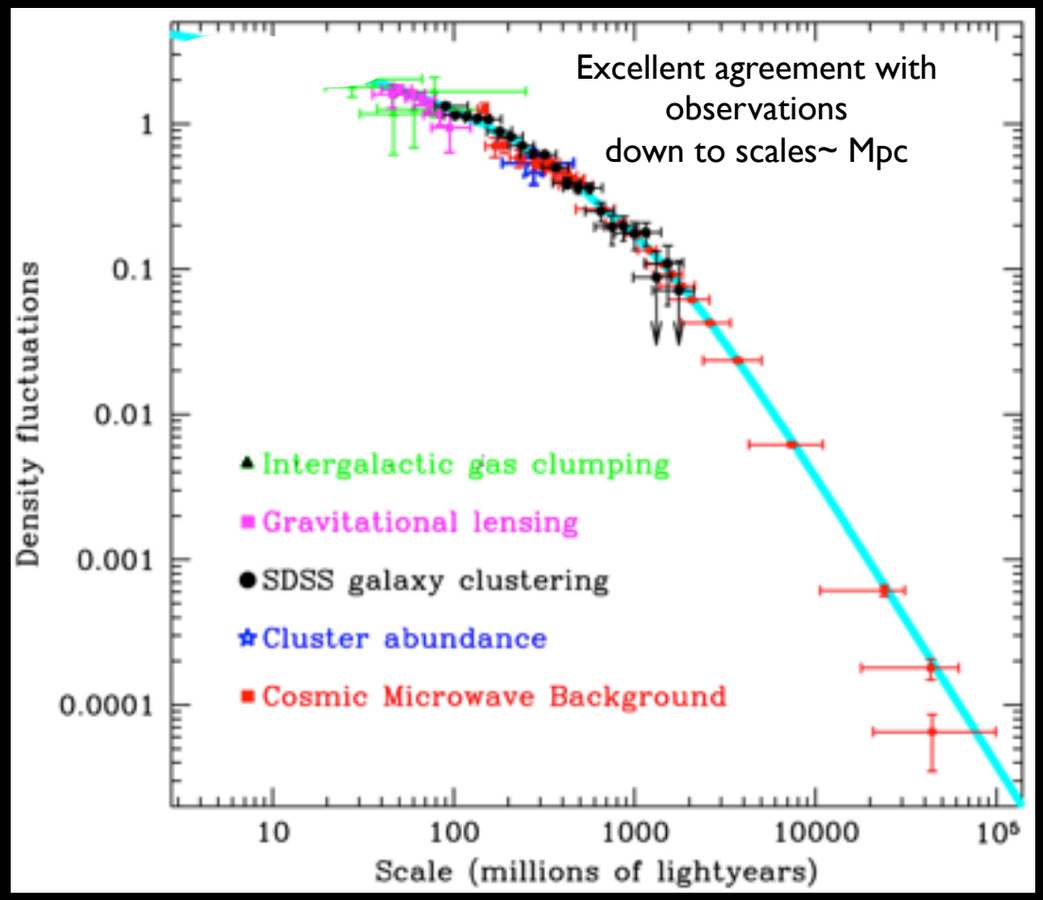

Springel et al. 2009

THE FRACTION OF QUIESCENT SATELLITE GALAXIES

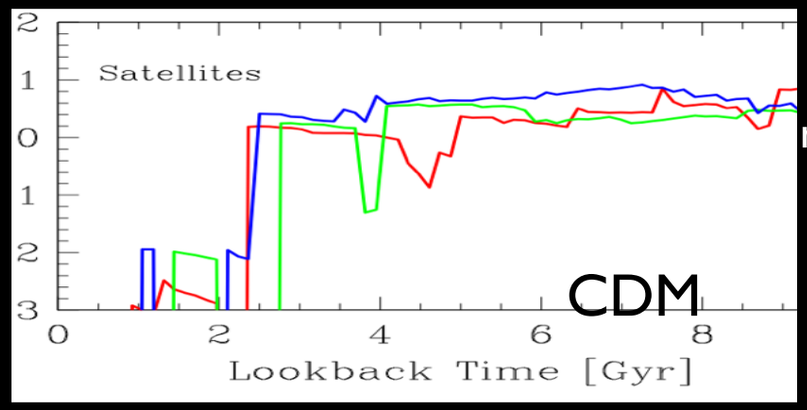

WDM delayed groth of
stellar mass
results into larger star formation
at low redshifts

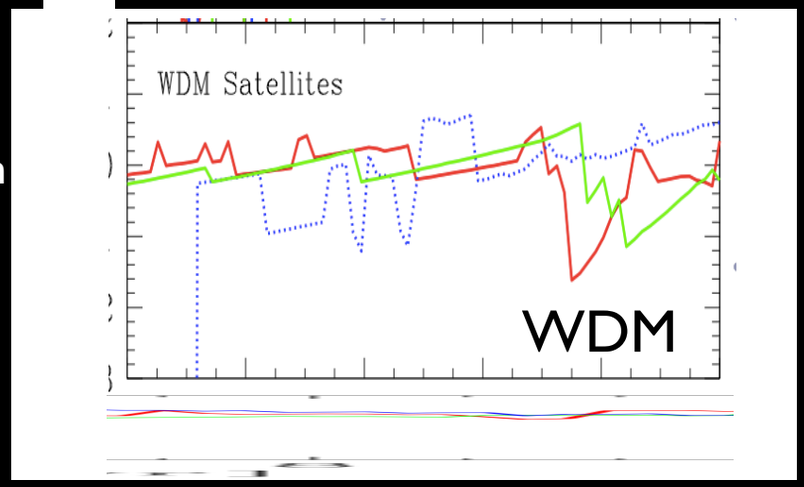

Specific Star Formation Rate

$$SSFR = \dot{M}_*/M*$$

Quiescent Fraction = fraction of galaxies with SSFR<10^{-11} yrs^{-1}

corresponds to minimum in the SSFR distribution

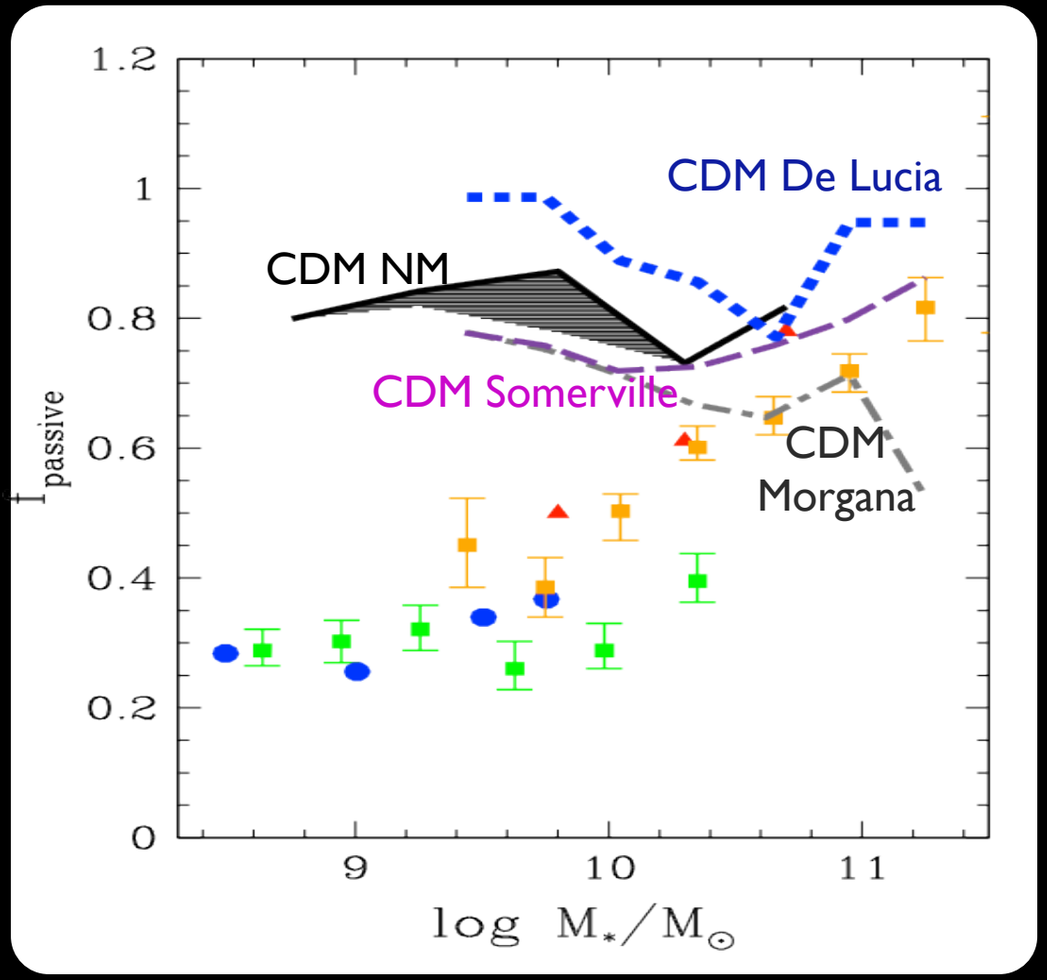

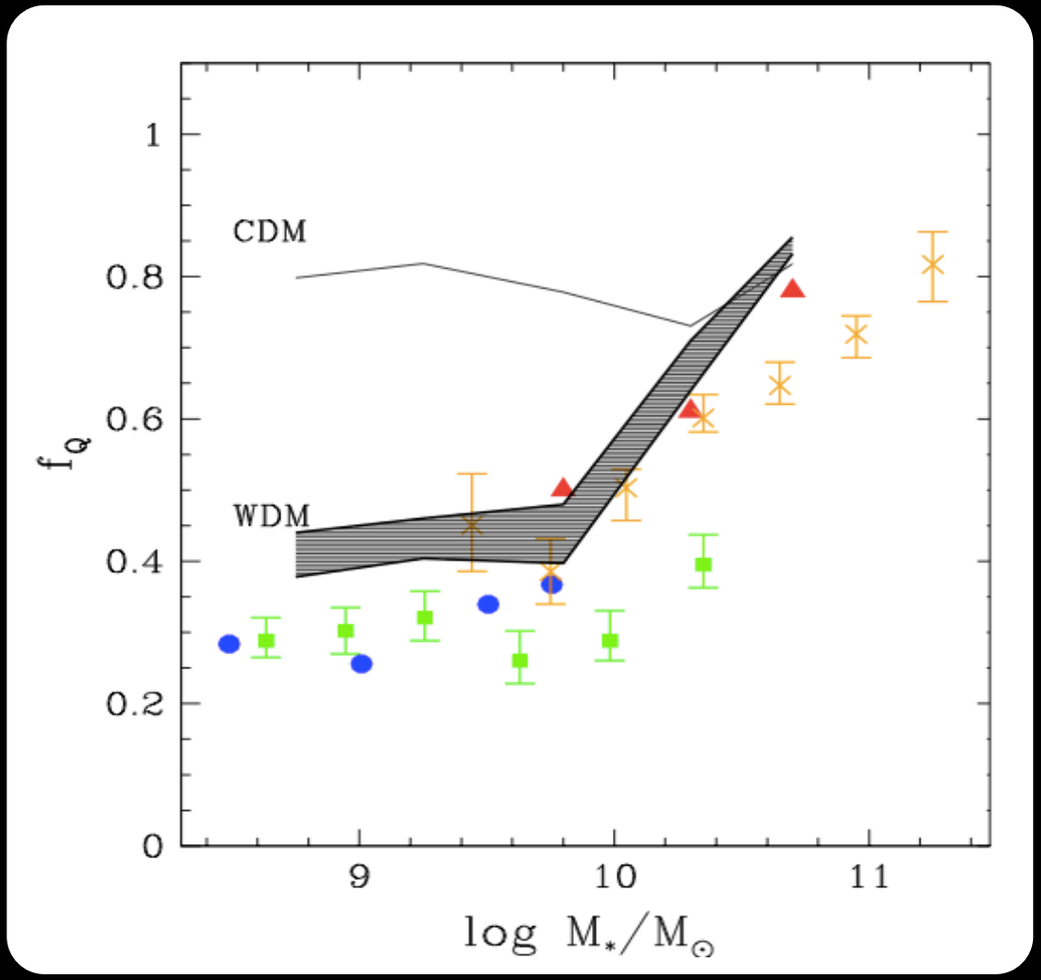

The M_*/M_h relation for low-mass galaxies

Enhancing the feedback results into inefficient star formation for given DM halo (suppress L/M).

In WDM the flatter shape of the LF allows for larger L/M ratios

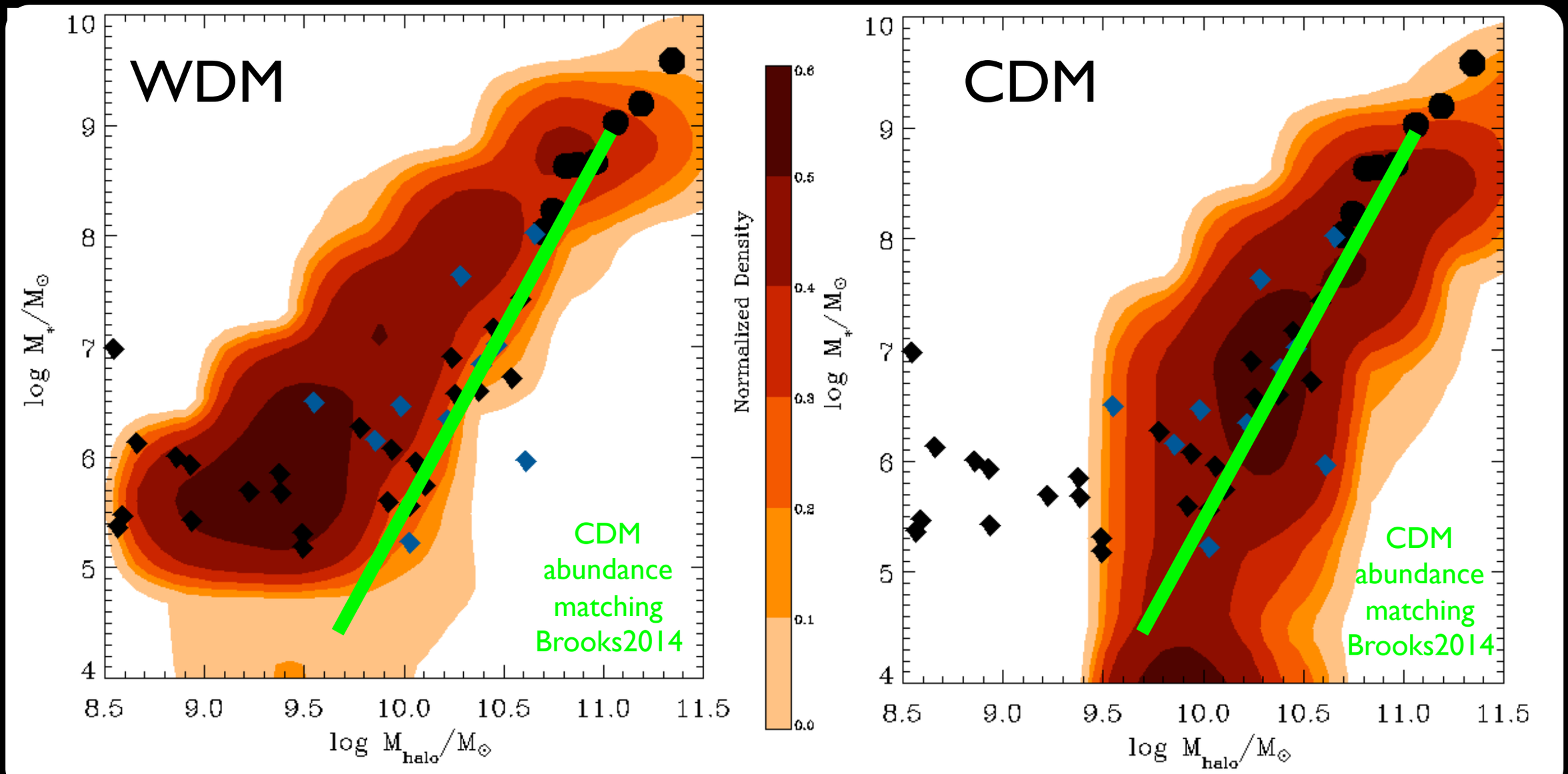

Hubble Frontier Field

The Frontier Fields Goals

Using Director's Discretionary (DD) observing time, HST is undertaking a revolutionary deep field observing program to peer deeper into the Universe than ever before and provide a first glimpse of JWST's universe.

These Frontier Fields will combine the power of HST with the natural gravitational telescopes of high-magnification clusters of galaxies. Using both the Wide Field Camera 3 and Advanced Camera for Surveys in parallel, HST will produce the deepest observations of clusters and their lensed galaxies ever obtained, and the second-deepest observations of blank fields (located near the clusters). These images will reveal distant galaxy populations ~10-100 times fainter than any previously observed, improve our statistical understanding of galaxies during the epoch of reionization, and provide unprecedented measurements of the dark matter within massive clusters.

This program is based upon the 2012 recommendations from the Hubble Deep Fields Initiative Science Working group: SWG Report 2012

Six Frontier Fields

Cluster Name	z	Cluster		Parallel Field	
		RA	Dec	RA	Dec
Year 1:					
Abell 2744	0.308	00:14:21.2	-30:23:50.1	00:13:53.6	-30:22:54.3
MACSJ0416.1-2403	0.396	04:16:08.9	-24:04:28.7	04:16:33.1	-24:06:48.7
Year 2:					
MACSJ0717.5+3745	0.545	07:17:34.0	+37:44:49.0	07:17:17.0	+37:49:47.3
MACSJ1149.5+2223	0.543	11:49:36.3	+22:23:58.1	11:49:40.5	+22:18:02.3
Year 3:					
Abell S1063 (RXCJ2248.7-4431)	0.348	22:48:44.4	-44:31:48.5	22:49:17.7	-44:32:43.8
Abell 370	0.375	02:39:52.9	-01:34:36.5	02:40:13.4	-01:37:32.8